Article:
Rastani, S., Keskin, M., Yüksel, T. et al. (2026) Uphill struggles, downhill gains: How road gradients and load dynamics influence electric vehicle routing decisions? European Journal of Operational Research, 333 (3). pp. 713-730. ISSN: 0377-2217

https://doi.org/10.1016/j.ejor.2026.01.020

European Journal of Operational Research

Uphill Struggles, Downhill Gains: How Road Gradients and Load Dynamics Influence Electric Vehicle Routing Decisions?

--Manuscript Draft--

Manuscript Number:	EJOR-D-24-03680R4
Article Type:	Theory and Methodology Paper
Section/Category:	(O) Routing
Keywords:	Electric vehicle routing, road gradient, regenerative braking, load-dependent, energy consumption
Corresponding Author:	Sina Rastani The University of Sheffield Management School Sheffield, UNITED KINGDOM OF GREAT BRITAIN AND NORTHERN IRELAND
First Author:	Sina Rastani
Order of Authors:	Sina Rastani
	Merve Keskin
	Tuğçe Yüksel
	Bülent Çatay
Abstract:	In this study, we investigate the Electric Vehicle Routing Problem with Time Windows incorporating partial recharges, factoring in energy consumption associated with road gradients, cargo weight, and the benefits of regenerative braking. Traversing arcs with positive road gradients demands more energy compared to flat networks. When an electric vehicle (EV) traverses uphill, energy consumption increases significantly, especially if it carries heavy loads, and can result in infeasible routes due to battery limitations. Conversely, as the EV travels downhill, gravity assists the vehicle's movement, allowing for gentler accelerator use or braking to maintain constant speed. Hence, energy can be recovered due to regenerative braking technology, resulting in energy savings and improved efficiency. We propose four different mathematical models and compare their performances. To assess the impact of road gradients, we generate a new dataset based on benchmark instances by assigning altitudes to each node in the network, employing clustering techniques to ensure consistency by adjusting node elevations relative to their cluster centers. We consider three terrain types characterized by progressively steeper average absolute road gradients. The results demonstrate that accounting for road gradients, cargo load, and regenerative braking significantly impacts routing decisions and can render the problem infeasible in networks with steep roads. While road gradients generally increase energy consumption, our findings indicate that in some instances, regenerative braking can improve the solution. This study underscores the importance of considering multiple factors affecting energy consumption to develop more effective transportation strategies for EVs.
Opposed Reviewers:	

Highlights

- Addressing the EVRP by adopting a realistic energy consumption model
- Energy consumption considers load, road gradients and regenerative braking
- Proposing different mathematical models enhanced with variable reduction and assessing their performances
- Generating a new dataset by associating nodes with altitudes consistently
- Investigating the impact of load and road network topography on routing decisions

Uphill Struggles, Downhill Gains: How Road Gradients and Load Dynamics Influence Electric Vehicle Routing Decisions?

Sina Rastani[a], Merve Keskin[a], Tuğçe Yüksel[b,c], Bülent Çatay[b,c]

[a] Management School University of Sheffield, Sheffield, UK

[b] Sabanci University, Faculty of Engineering and Natural Sciences, Istanbul, Turkey

[c] Smart Mobility and Logistics Lab, Sabanci University, Istanbul, Turkey

Abstract

In this study, we investigate the Electric Vehicle Routing Problem with Time Windows incorporating partial recharges, factoring in energy consumption associated with road gradients, cargo weight, and the benefits of regenerative braking. Traversing arcs with positive road gradients demands more energy compared to flat networks. When an electric vehicle (EV) traverses uphill, energy consumption increases significantly, especially if it carries heavy loads, and can result in infeasible routes due to battery limitations. Conversely, as the EV travels downhill, gravity assists the vehicle's movement, allowing for gentler accelerator use or braking to maintain constant speed. Hence, energy can be recovered due to regenerative braking technology, resulting in energy savings and improved efficiency. We propose four different mathematical models and compare their performances. To assess the impact of road gradients, we generate a new dataset based on benchmark instances by assigning altitudes to each node in the network, employing clustering techniques to ensure consistency by adjusting node elevations relative to their cluster centers. We consider three terrain types characterized by progressively steeper average absolute road gradients. The results demonstrate that accounting for road gradients, cargo load, and regenerative braking significantly impacts routing decisions and can render the problem infeasible in networks with steep roads. While road gradients generally increase energy consumption, our findings indicate that in some instances, regenerative braking can improve the solution. This study underscores the importance of considering multiple factors affecting energy consumption to develop more effective transportation strategies for EVs.

Keywords: Electric vehicle routing, road gradient, regenerative braking, load-dependent, energy consumption

1. Introduction

Studying different factors that affect energy consumption is often neglected in the Vehicle Routing Problem literature since it may bring more complexity to the problem, or it may not be an important issue as the internal combustion engine vehicles (ICEVs) do not need to refuel frequently and the refueling process is fast. Nevertheless, given the limited battery capacity of electric vehicles (EVs) and their time-consuming recharging processes, it is essential to consider these factors in the Electric Vehicle Routing Problem

(EVRP) literature to ensure accurate and efficient routing solutions.

The first study that considered an EV fleet for freight transportation was conducted by Conrad and Figliozzi (2011), where EVs could recharge at selected customer locations. Erdoğan and Miller-Hooks (2012) introduced the Green Vehicle Routing Problem where the fleet consists of alternative fuel vehicles (AFVs). In their study, AFVs were allowed to refuel at public alternative fueling stations (AFSs). The fuel tank was assumed to be fully filled at a constant time. Schneider et al. (2014) presented the Electric Vehicle Routing Problem with Time Windows (EVRPTW) by assuming a full recharge strategy. They formulated a mathematical programming model of the problem and developed a hybrid metaheuristic approach that combined the variable neighborhood search (VNS) and tabu search (TS) methods. They also proposed a new dataset based on well-known Solomon (1987) instances generated for the VRPTW. Bruglieri et al. (2015) and Keskin and Çatay (2016) relaxed the assumption of full recharge. The former proposed a VNS Branching method to solve small problems, whereas the latter developed an adaptive large-neighborhood search method that could efficiently solve large-size problems. Desaulniers et al. (2016) considered four recharging cases, namely, full and partial strategies allowing single and multiple recharges en route, and proposed an exact method based on the branch-price-and-cut approach. Recently, Duman et al. (2022) also used branch-price-and-cut to develop both exact and heuristic methods and presented new best solutions for the same problem.

Several EVRP variants have been addressed in the literature, including fleet composition (Goeke and Schneider, 2015; Macrina et al., 2019; Hiermann et al., 2019; Wang and Zhao, 2022; Bruglieri et al., 2025), multiple charging technologies (Felipe et al., 2014; Keskin and Çatay, 2018; Zhang et al., 2024), nonlinear charging function (Montoya et al., 2017; Zhang et al., 2021; Park and Lee, 2024), battery swapping (Yang and Sun, 2015; Jie et al., 2019; Raeesi and Zografos, 2022; Çatay and Sadati 2023; Zhang et al., 2024; Souza et al., 2024), electrified roads (Gutierrez-Alcoba et al., 2023; Akbari et al., 2024), battery degradation and depletion (Pelletier et al., 2017; Soysal et al., 2020; Zhang et al., 2021; Zang et al., 2022), location routing (Schiffer and Walther, 2017; Çalık et al., 2021; Guo et al., 2022), two-echelon routing (Jie et al., 2019), availability of recharging stations and stochastic recharging times (Sweda et al., 2017; Keskin et al., 2019; Kullman et al., 2020; Keskin et al., 2021; Bruglieri et al., 2021; Froger et al., 2022; Lam et al., 2022; Dastpak et al., 2024), flexibility in deliveries (Sadati et al., 2022), time dependent routing (Basso et al., 2021; Zhang et al., 2023), and presence of soft time windows (Liu et al., 2023; Sun et al., 2025). Some recent studies optimize routing and recharging scheduling at the stations simultaneously due to the limited number of chargers (Wang and Zhao, 2023; Yamín et al., 2024; Ma et al., 2024; Bragin et al., 2024; Dastpak et al., 2024). Erdelić and Carić (2019), Kucukoglu et al. (2021) and Xiao et al. (2021) provided a comprehensive review of the EV technology and a survey of EVRP variants, while Dolgui et al. (2024)

presented a review for the EV charging scheduling problems including those combined with routing.

Energy consumption on the road is influenced by various factors beyond just the distance traveled. There are several studies considering the internal factors such as the vehicle's weight (Kancharla and Ramadurai, 2020; Rastani and Çatay, 2023; Liu et al., 2023; Sun et al., 2025), velocity (Basso et al., 2021; Zhang et al., 2023; Erdoğan et al., 2023; Bruglieri et al., 2023), as well as the external factors such as ambient temperature (Rastani et al., 2019; Wang et al., 2023; Li et al., 2024). Furthermore, road gradient is another external factor that can affect the energy consumption. Among these factors, road gradient and the weight of the transported cargo can significantly influence routing decisions (Basso et al., 2019; Basso et al., 2021). The real road network of the cities where the logistic companies operate may not be flat. Traveling on a road with a positive gradient requires more energy compared to a road on a flat network. Furthermore, when an EV carries heavy load, the effect of road gradients on the energy consumption intensifies since moving uphill with heavy load requires even more energy to complete the journey. On the other hand, if an EV traverses a road with a negative gradient, the driver may need to either push the accelerator pedal more gently due to the gravity assisting the vehicle's movement or apply the brake to maintain a constant speed. This braking action releases energy, which can be captured and stored in the battery through regenerative braking (Xu et al., 2011, Wu et al., 2015).

Companies dealing with heavy loads and operating in non-flat terrain are particularly affected by road gradients and cargo weight. For these businesses, a model that accounts for these factors can yield more effective transportation strategies compared to basic routing models. Motivated by this need for more accurate and practical models, we address the load-dependent EVRPTW by taking into account the effect of road gradients and regenerative braking on energy consumption, which we refer to as the EVRPTW-GR. To the best of our knowledge, this is the first study to examine the role of these factors on fleet sizing, battery recharging, and routing decisions in the context of EVRPs.

Table 1 summarizes recent studies that calculate energy consumption in a more realistic manner by incorporating factors such as load, speed, road gradients, and energy recuperation. The last column of the table indicates the solution methodology employed, where (A)LNS, ACO, RKS, and ILS refer to (Adaptive) Large Neighborhood Search, Ant Colony Optimization, Random Kernel Search, and Iterative Local Search, respectively. "MILP" is used to denote studies that report results solely from a mixed-integer linear programming solver. While many of these studies consider one or two of the aforementioned factors, they often focus on a less constrained routing problems, such as those without en-route recharging, those requiring full recharging at stations, or those lacking time window constraints. A key distinguishing feature, addressed by only one prior study, is the inclusion of regenerative braking and the associated energy recovery influenced by vehicle load and road slope. The most comparable study is Basso et al. (2019).

However, their approach includes an approximation: in the first stage, a linear energy consumption function is constructed using a fixed weight; routing decisions are then made based on the coefficients of this approximation in the next stage. In contrast, our study differs by explicitly accounting for the current total weight of the vehicle during the routing phase, leading to a more accurate representation of energy consumption.

Table 1. Overview of the related EVRP literature

	Calculation							
Paper	Load	Speed	Gradient	Energy Recuperation	En-route Charging	TWs	Problem Name	Solution Method
Goeke and Schneider (2015)	✓				Full	✓	EVRP with Time Windows and Mixed Fleet	ALNS
Zhang et al. (2018)	✓				Full	-	Electric Vehicle Routing Problem	ACO
Kancharla and Ramadurai (2018)	✓				Full	✓	EVRP with Time Windows	ALNS
Basso et al. (2019)	✓	✓	✓	✓	Full	✓	Two-stage EVRP	MILP
Xiao et al. (2019)	✓	✓			-	✓	EVRP with Time Windows Considering the Energy/Electricity Consumption Rate	MILP
Macrina et al. (2019)					Partial	✓	Green Vehicle Routing Problem	LNS-based matheuristic
Kancharla and Ramadurai (2020)	✓				Partial	-	E-VRP with Non-Linear charging and Load-Dependent Discharging	ALNS
Bruglieri et al. (2023)	✓	✓			Partial	✓	EVRP with Time Windows and Realistic Energy Consumption Rate	RKS matheuristic
Erdoğan et al. (2023)		✓			Partial	-	Energy Efficient Path Problem for Plug-in Electric Vehicles	ILS
Liu et al. (2023)	✓	✓			Full	Soft	EVRP with Variable Vehicle Speed and Soft Time Windows	Adaptive Hybrid ACO
Rastani and Çatay (2023)	✓				Partial	✓	Load-Dependent EVRP with Time Windows	LNS-based matheuristic
Sun et al. (2025)	✓				Full	Soft	EVRP that Considers Soft Time Windows and Linear Weight-Related Discharging	ALNS
This paper	✓		✓	✓	Partial	✓	EVRPTW with Road Gradients and Regenerative Braking	MILP

In line with the existing literature, we adopt a hierarchical objective function. The primary objective is to minimize the fleet size, while the secondary objective is to minimize the total energy consumption. To formulate this problem, we propose four different mathematical models with different characteristics. As this problem has not been studied before, we generate dataset based on benchmark instances from the literature by assigning altitudes to each node in the network. Clustering techniques are employed to ensure a consistent dataset by adjusting node elevations based on their proximity to the cluster center. Using this dataset, we then solve the models using Gurobi and compare their performances. We present results from three different terrain types, each with progressively steeper average absolute road gradients, which represent networks with different steepness characteristics. Our results provide several managerial insights that logistics companies may benefit in their decision-making processes from strategic to operational levels.

The key contributions of this paper are fourfold. First, we introduce the EVRPTW-GR and provide its

general (nonlinear) mathematical formulation. Second, we propose three alternative mixed-integer linear programming (MILP) formulations and compare their performances. Third, we generate a new dataset by consistently assigning altitudes to the nodes in benchmark instances from the literature. Finally, we conduct an extensive computational study to demonstrate the critical importance of accounting for road gradients and cargo load in routing decisions.

The remainder of the paper is organized as follows: Section 2 introduces the problem and presents the nonlinear programming model. Section 3 then provides three linear programming models to formulate the problem, including an approximation to the first model as well as its linearized counterparts. Section 4 presents the details of data generation, experimental study and discusses the results. Finally, concluding remarks are provided in section 5.

2. Problem description and formulation

The EVRPTW-GR deals with a homogeneous fleet of EVs that are dispatched from a single depot to serve a set of customers with known demands, time windows, and service times. We assume that EVs travel at a constant speed, and they may stop by the recharging stations to replenish energy as much as needed to continue their routes. The recharging function has a nonlinear behavior, e.g., recharging time increases nonlinearly with respect to the energy amount, as the terminal voltage and charging current change during the recharging process, which involves two phases (Pelletier et al., 2017). In the first phase, the charging current is held constant, in which the energy is transferred at a linear rate with respect to time, until the terminal voltage of the battery reaches to a maximum value. In the second phase, the terminal voltage is held constant at that maximum value, which makes the charging current decrease exponentially. Hence, battery state of charge (SoC) increases concavely in this phase (Marra et al., 2012). Despite this nonlinear behaviour of the recharging function, it is a common practice to operate within the first phase of recharging to prolong the battery life (Pelletier et al., 2017). Therefore, we adopt this approach where the recharging time is proportional to the energy amount received at the station. In addition, we allow the EVs to recharge at most once between two consecutive customers, which is more practical in last-mile logistics.

An arc between two nodes represents a shortest path between them and the road gradient between the nodes is assumed to be the average gradient of that path. The energy consumption of the EVs depends on road gradient, regenerative braking, and freight load in addition to the distance traveled. While traveling downhill, e.g., on arcs with a negative gradient, the driver either needs to push the accelerator pedal more gently due to the gravity helping the vehicle to move more easily, or the driver can take the foot off the accelerator pedal, or even push the brake pedal to keep the vehicle speed constant, which recovers some energy from braking. This is called regenerative braking as the released energy can be saved in the battery,

thus creating a negative consumption. In the former case, the vehicle still consumes energy from the battery, but it is less than that on a flat road. On the other hand, traveling uphill, e.g., on arcs with a positive gradient, requires more energy compared to flat and downhill roads. These different patterns of energy consumption are further affected by the current weight of the vehicle. Therefore, the objective is to find the routes of the EVs such that the total energy consumption is minimized, taking into consideration the loads of the vehicles and the gradients of the arcs. EVs depart from the depot, where they can recharge their batteries overnight. Unlike previous studies, EVs do not necessarily need to fully recharge their batteries before departure. This is because they can regenerate energy through regenerative braking if they immediately encounter a downhill arc upon leaving the depot.

Figure 1 presents a toy example illustrating how considering road gradients affect optimal route planning and energy consumption on an instance with a single depot, denoted by "0", eight customers and four recharging stations. We consider two scenarios with respect to road gradients: The first ignores the road gradients for each arc in the network when planning the routes, while the second takes them into account in routing decisions. In both scenarios, the distance matrices are symmetric. However, when road gradients are considered, the energy consumed while traveling on an arc change depending on the gradient, which makes the energy consumption network asymmetric in the second scenario. The solutions obtained for these scenarios, which take into account the effect of cargo load in both, are illustrated in Figures 1.a and 1.b. The solid and dashed arcs represent the roads with positive and negative gradients, respectively. The numbers on the arcs represent the amount of energy consumed to travel along that arc, whereas in Figure 1.b, the numbers in parentheses next to the arcs indicate the road gradients in percentages. For each route, the total distance traveled and energy consumption are shown as "Distance" and "Energy", respectively, and the battery capacity of the EVs is 77.8.

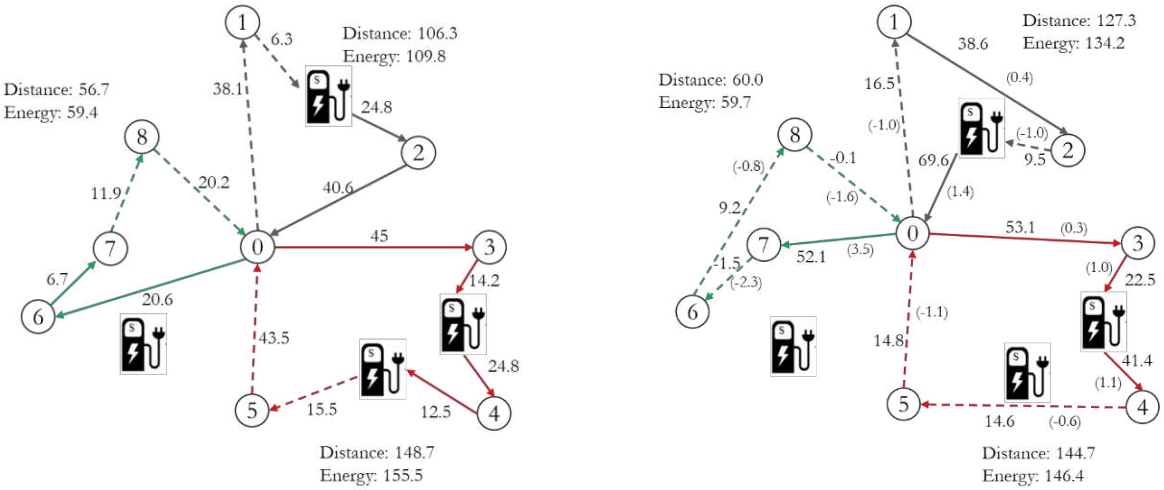

(a) Ignoring road gradients

(b) Considering road gradients

Figure 1. Illustration of how optimal route plans change when road topographies are considered.

The red route in Figure 1.a demonstrates that on a flat network, the EV requires two station visits to complete its tour. As shown in Figure 1.b, arcs (4, 5) and (5, 0) have a slightly negative gradient and the EV can traverse them by consuming less energy compared to the first scenario, where road gradients are ignored. Hence, the EV does no longer need to recharge at two stations as one station visit is sufficient to complete the tour. This results in a reduced total distance and energy consumption, which are decreased by about four and nine units, respectively. Notably, if the gradients on these arcs were steeper, the EV could even regenerate energy through braking.

However, road gradients do not always benefit routing plans; in fact, they often increase energy consumption and necessitate more frequent visits to recharging stations. This is demonstrated in the black route. In Figure 1.b, where road gradients are considered, the EV must travel approximately 21 units more distance as the route obtained in the first scenario, which ignores the road gradients, is no longer feasible due to the steep roads on the arcs (station, 2) and (2,0). This results in a changed order of visiting the station, which requires about 24 units higher energy compared to the scenario where road gradients are ignored. It is evident that steeper roads may necessitate more frequent visits to recharging stations.

In the green route, we observe that considering road gradients can alter the optimal sequence of customer visits. When road gradients are considered but the sequence from first scenario is maintained, the EV must visit a station and recharge en route to complete the tour. This detour increases the distance traveled and energy consumption by 12.6 and 11 units, respectively. This is why in the scenario considering the road gradients, the order of customer visits slightly changes so that the EV benefits from regenerative braking, which saves energy on arcs (7, 6) and (8, 0). The resulting total energy consumption is approximately 0.3 units higher than that in the first scenario, but it is much better than an increase of 11 units. Considering road gradients in route planning could save approximately 9.3 units of distance and 10.7 units of energy consumption.

This example with different effects that the road gradients can cause demonstrate that a steep network can alter the sequence of visits, require additional station visits for recharging along the tour, or eliminate unnecessary station visits. Therefore, to achieve the optimal route plans, it is essential to consider road gradients along with other factors such as load and time windows.

2.1. Energy consumption function

The energy consumption of an EV depends on several factors such as its shape, mass, road gradient, acceleration, etc. To find the required energy to travel on an arc, one needs to calculate the power demand of the vehicle, which can be obtained by using tractive power requirements placed on the vehicle at the wheels. The tractive power P_{tract} is calculated (in kW) as follows (Barth et al., 2005; Barth and

Boriboonsomsin, 2009):

$$F = Ma + Mgsin\theta + 0.5C_d\rho Av^2 + MgC_rcos\theta \quad (1)$$

$$P_{tract} = \frac{Fv}{1000} \quad (2)$$

where Equation (1) calculates the tractive effort F using the total mass (M in kg) of the vehicle including its curb weight (w) and the cargo weight, the acceleration of the vehicle (a in m/sec^2), the gravitational constant (g in m/sec^2), the road angle (θ in degrees), the coefficient of aerodynamic drag (C_d), the air density (ρ in kg/m^3), the frontal area of the vehicle (A in m^2), the speed (v in $\mathrm{m/s}$), and the coefficient of rolling resistance (C_r).

Considering the tractive power function in Equation (2), if the road gradient is positive, the tractive power will have a positive value. However, if the road gradient is negative, there are two possible outcomes for the tractive power. If $(Ma + 0.5C_d\rho Av^2 + MgC_rcos\theta) \geq |Mgsin\theta|$, the tractive power will be positive, meaning that the vehicle consumes energy while traveling. On the other hand, if the road is steeper and $(Ma + 0.5C_d\rho Av^2 + MgC_rcos\theta) < |Mgsin\theta|$, then the tractive power will be negative, and thus the vehicle can save energy using the regenerative braking technology. Since the total weight of the vehicle changes while traveling as it collects goods from customers, the tractive power needed on arc (i, j) is represented as a function of the current weight of the vehicle M_{ij}, i.e., $P_{tract}(M_{ij})$. Hence, it is the current weight of the vehicle and the road gradient that determines whether the energy is consumed or gained while traveling on a specific road segment. To simplify notation, let us define $\beta_{ij} = \frac{(sin\theta_{ij} + C_r cos\theta_{ij})gv}{1000}$, and $\gamma = \frac{0.5C_d\rho Av^3}{1000}$. Then the tractive power function needed on arc (i, j) can be presented as equation (3).

$$P_{tract}(M_{ij}) = M_{ij}(a + \beta_{ij}) + \gamma \quad (3)$$

When the tractive power is positive, it can be converted to second-by-second battery power output (P in kW) in Equation (4). On the other hand, if the tractive power is negative, the second-by-second battery power output is calculated using Equation (5) (Asamer et al., 2016; Fiori et al., 2016). Note that in this study we neglect the power demand associated with the accessory equipment, such as air conditioning, audio system, and cabin lights.

$$P = \frac{P_{tract}(M_{ij})}{\mu} \qquad P_{tract}(M_{ij}) \geq 0 \quad (4)$$

$$P = \mu_r . P_{tract}(M_{ij}) \qquad P_{tract}(M_{ij}) < 0 \quad (5)$$

where the vehicle's drivetrain efficiency is shown by μ, which includes the energy losses between the electric motor and battery, the energy losses in transforming energy to the wheels, as well as electric battery

efficiency. μ_r includes the factors in μ as well as efficiency of the regenerative braking process, as only a proportion of the regenerated energy can be saved in the battery.

Finally, the energy consumption on an arc (in kWh/km), $P/\overline{V}$ is calculated by either Equations (6) or (7) depending on the tractive power requirement on that arc, where $\overline{V}$ is the vehicle speed (in km/h). Since the tractive power $P_{tract}(M_{ij})$ depends on the current weight of the vehicle, the energy consumption while traversing arc (i,j) is also a function of the vehicle weight, and hence represented as $h_{ij}(M_{ij})$. If Equation (6) is used, then $h_{ij}(M_{ij})$ is the amount of energy consumed from the battery, otherwise, that is the energy amount received back in the battery by regenerative braking calculated in Equation (7). Note that the distance between nodes i and j is denoted by d_{ij}.

$$h_{ij}(M_{ij}) = \frac{d_{ij}P_{tract}(M_{ij})}{\mu\overline{V}} \qquad \text{if } P_{tract}(M_{ij}) \geq 0 \tag{6}$$

$$h_{ij}(M_{ij}) = \frac{\mu_r d_{ij}P_{tract}(M_{ij})}{\overline{V}} \qquad \text{if } P_{tract}(M_{ij}) < 0 \tag{7}$$

2.2. Model formulation

We formulate EVRPTW-GR following the mathematical notation and modeling convention in the literature (Schneider et al., 2014; Keskin and Çatay, 2016). Let V and F be the set of customers and the set of recharging stations, respectively. 0 and $n+1$ denote the two copies of the depot where EVs start and end their tours. We define $V_0 = V \cup \{0\}$, $V_{n+1} = V \cup \{n+1\}$, $V_{0,n+1} = V \cup \{0\} \cup \{n+1\}$, $V' = V \cup F$, $V_0' = V_0 \cup F$, and $V_{n+1}' = V_{n+1} \cup F$. Then, the problem can be represented on a complete directed graph $G = (N, A)$ with the set of arcs $A = \{(i,j) | i,j \in N, i \neq j\} \backslash \{(i,j): i,j \in F\}$ in which origin and destination nodes are not stations at the same time, and $N = V_{0,n+1} \cup F$ is the set of all nodes in the network.

Each customer $i \in V$ has a positive demand q_i, a service time s_i, and a time window $[e_i, l_i]$, where e_i and l_i denote the earliest and latest times customer i can be visited, respectively. All EVs have a cargo capacity of C and a battery capacity of Q. At each recharging station, one unit of energy is transferred in r time units. Travel time from customer i to customer j is denoted by t_{ij} if the journey is direct. If a recharging station s is visited in between, $\hat{t}_{ijs} = t_{is} + t_{sj} - t_{ij}$ is defined as the additional travel time compared to a direct trip. Note that $\hat{t}_{ijs}$ does not include the recharging time at station s. M_{ij} keeps track of the gross weight of the vehicle when traveling from customer i to j. If a station $s \in F$ is visited in between, the weight after the departure from the station is represented by $\widehat{M}_{ijs}$. Note that, this is an auxiliary variable to be able to calculate the extra energy consumption if a station is visited between the customers. As there is no collection at stations, $\widehat{M}_{ijs}$ should be equal to M_{ij}.

Table 2. Mathematical notation

Sets:	
V	Set of customers
V_0	Set of customers and departure depot
V_{n+1}	Set of customers and arrival depot
V'_0	Set of customers, stations, and departure depot
V'_{n+1}	Set of customers, stations, and arrival depot
$V_{0,n+1}$	Set of customers, departure, and arrival depots
F	Set of recharging stations
F_0	Set of recharging stations and the departure depot, i.e., $F_0 = F \cup \{0\}$
F_{n+1}	Set of recharging stations and the arrival depot, i.e., $F_{n+1} = F \cup \{n+1\}$
N	Set of customers, stations, arrival and departure depots
A	Set of arcs, in which origin and destination nodes are not stations at the same time, i.e., $A = \{(i,j) \mid i,j \in N, i \neq j\} \backslash \{(i,j): i,j \in F\}$
Parameters:	
t_{ij}	Travel time from node i to node j, $i,j \in N$
$\hat{t}_{ijs}$	Additional trip time for visiting station $s \in F$ between customers $i,j \in V$ $\left(\hat{t}_{ijs} = t_{is} + t_{sj} - t_{ij}\right)$
q_i	Demand of customer $i \in V$
s_i	Time required to serve customer $i \in V$
$[e_i, l_i]$	Service time window associated with node $i \in N$
C	Cargo capacity of the vehicles
Q	Battery capacity of the vehicles
r	Recharging rate
U	A large positive scalar
n	Number of available EVs
Decision variables:	
τ_i	Service start time at node $i \in N$
M_{ij}	Gross weight of the vehicle while traveling from $i \in V_0$ to $j \in V_{n+1}$
$\widehat{M}_{ijs}$	Gross weight of the vehicle at departure from station $s \in F$ if it travels from $i \in V_0$ to $j \in V_{n+1}$ through station $s \in F$
y_i	Battery SoC of the vehicle upon arrival at or departure from node $i \in V_{0,n+1}$
y_{ijs}	Battery SoC of the vehicle upon arrival at station $s \in F$ on route (i,s,j), $i \in V_0, j \in V_{n+1}$
Y_{ijs}	Battery SoC of the vehicle at departure from station $s \in F$ on route (i,s,j), $i \in V_0, j \in V_{n+1}$
x_{ij}	1 if the vehicle travels from node $i \in V_0$ to node $j \in V_{n+1}$; 0 otherwise
z_{ijs}	1 if the vehicle recharges at station $s \in F$ while traveling from $i \in V_0$ to $j \in V_{n+1}$; 0 otherwise

If a vehicle travels from customer i to customer j, the binary decision variable x_{ij} takes value one. If a station $s \in F$ is visited in between, the binary decision variable z_{ijs} takes value one. y_i keeps track of the battery SoC at arrival at node $i \in V_{0,n+1}$. However, the battery SoC at arrival at and departure from the stations is controlled by y_{ijs}, and Y_{ijs}, respectively. τ_i denotes the time when the service starts at node $i \in N$. The energy consumption function along arc (i,j), $h_{ij}(M_{ij})$ is calculated by either Equations (6) or (7) depending on the sign of the tractive power, $P_{tract}(M_{ij})$, which is influenced by the road gradient and

weight of the vehicle. This dependency introduces conditional statements, resulting in a nonlinear relationship between the variables and we name this model as NL-Model. The sets, parameters, and decision variables employed in model formulation are summarized in Table 2.

Having defined the parameters and decision variables, NL-Model is formulated as follows:

$$\text{Min} \sum_{i \in V'_0} \sum_{j \in V'_{n+1}} h_{ij}\left(M_{ij}\right) \tag{8}$$

subject to

$$\sum_{\substack{j \in V_{n+1} \\ j \neq i}} x_{ij} = 1 \qquad \forall\, i \in V \tag{9}$$

$$\sum_{\substack{i \in V_0 \\ i \neq j}} x_{ij} - \sum_{\substack{i \in V_{n+1} \\ i \neq j}} x_{ji} = 0 \qquad \forall\, j \in V \tag{10}$$

$$\sum_{s \in F} z_{ijs} \leq x_{ij} \qquad \forall\, i \in V_0, j \in V_{n+1}, i \neq j \tag{11}$$

$$\tau_i + \left(t_{ij} + s_i\right)x_{ij} + \sum_{s \in F}\left(\hat{t}_{ijs} z_{ijs} + r\left(Y_{ijs} - y_{ijs}\right)\right) - l_0\left(1 - x_{ij}\right) \leq \tau_j \qquad \forall\, i \in V_0, j \in V_{n+1}, i \neq j \tag{12}$$

$$e_j \leq \tau_j \leq l_j \qquad \forall\, j \in N \tag{13}$$

$$M_{0j} = w x_{0j} \qquad \forall\, j \in V_{n+1} \tag{14}$$

$$\sum_{\substack{i \in V_0 \\ i \neq j}} M_{ij} + q_j x_{jk} - (w + C)\left(1 - x_{jk}\right) \leq M_{jk} \leq \sum_{\substack{i \in V_0 \\ i \neq j}} M_{ij} + q_j x_{jk} + (w + C)\left(1 - x_{jk}\right) \qquad \forall\, j \in V, k \in V_{n+1}, j \neq k \tag{15}$$

$$(w + q_i)x_{ij} \leq M_{ij} \leq \left(w + \sum_{i \in V} q_i\right)x_{ij} \qquad \forall\, i \in V, j \in V_{n+1}, i \neq j \tag{16}$$

$$\widehat{M}_{0js} = w z_{0js} \qquad \forall\, j \in V_{n+1}, s \in F \tag{17}$$

$$\sum_{\substack{i \in V_0 \\ i \neq j}} M_{ij} + q_j z_{jks} - (w + C)\left(1 - z_{jks}\right) \leq \widehat{M}_{jks} \leq \sum_{\substack{i \in V_0 \\ i \neq j}} M_{ij} + q_j z_{jks} + (w + C)\left(1 - z_{jks}\right) \qquad \forall\, j \in V, k \in V_{n+1}, s \in F, j \neq k \tag{18}$$

$$w \leq \widehat{M}_{ijs} \leq \left(w + \sum_{i \in V} q_i\right) z_{ijs} \qquad \forall\, i \in V, j \in V_{n+1}, s \in F, i \neq j \tag{19}$$

$$0 \leq y_j \leq y_i - h_{ij}\left(M_{ij}\right) + U\left(1 - x_{ij} + \sum_{s \in F} z_{ijs}\right) \qquad \forall\, i \in V_0, j \in V_{n+1}, i \neq j \tag{20}$$

$$0 \leq y_{ijs} \leq y_i - h_{is}(M_{ij}) + U(1 - z_{ijs}) \qquad \forall\, i \in V_0, j \in V_{n+1}, s \in F, i \neq j \qquad (21)$$

$$y_j \leq Y_{ijs} - h_{sj}(M_{ij}) + U(1 - z_{ijs}) \qquad \forall\, i \in V_0, j \in V_{n+1}, s \in F, i \neq j \qquad (22)$$

$$y_{ijs} \leq Y_{ijs} \leq Q z_{ijs} \qquad \forall\, i \in V_0, j \in V_{n+1}, s \in F, i \neq j \qquad (23)$$

$$y_j \leq Q \qquad \forall\ j \in V_{0,n+1} \qquad (24)$$

$$x_{ij} \in \{0,1\} \qquad \forall\, i \in V_0, j \in V_{n+1}, i \neq j \qquad (25)$$

$$z_{ijs} \in \{0,1\} \qquad \forall\, i \in V_0, j \in V_{n+1}, s \in F, i \neq j \qquad (26)$$

The objective function (8) minimizes the total energy consumption using the energy consumption function $h_{ij}(M_{ij})$, which is calculated by either Equations (6) or (7). The connectivity of customer visits is imposed by constraints (9), whereas the flow conservation at each vertex is ensured by constraints (10). Constraints (11) link the variables x_{ij} and z_{ijs} and make sure that if arc (i,j) is not traversed, a station cannot be visited in between. Constraints (12) keep track of the time while traveling from node i to node j, where l_0 denotes the latest time that the EVs should return to the depot. Note that, if a station is visited in between, the recharging time at the station and the detour time to stop by the station are also considered through z_{ijs} variables. Constraints (13) impose the service time window restriction. Since this is a pick-up problem, the total weight of the vehicle when departing from the depot is equal to the curb weight, which is ensured by constraints (14), and it is updated by constraints (15) throughout its journey. Constraints (16) set the limits for the total weight of the vehicle while traveling on arc (i,j), considering the demands of the customers. Constraints (17) – (19) are similar to constraints (14) – (16) and keep track of the vehicle weight in case a station is visited between nodes i and j. Note that constraints (16) and (19) set the weight of the EV to zero, if it does not travel from customer i to customer j. Hence, corresponding consumption value is zero. Constraints (20) – (24) keep track of the battery SoC at each node and make sure that it never falls below zero or exceeds the battery capacity, Q, where $U = Q + \ max_{(i,j)\in A}\{h_{ij}(M_{ij})\}$. Constraints (20) establish the battery SoC consistency if the vehicle travels from node i to node j directly. If a recharging station is visited in between, constraints (20) become redundant, and constraints (21) and (22) calculate the battery SoC upon arrival at the station and at the node visited after the station, respectively. Constraints (23) and (24) set the limits for battery SoC when the vehicle arrives at or departs from a station and a customer or the depot, respectively. Constraints (25) and (26) define the domain of the decision variables.

2.3. Variable reduction

In this section, we describe a series of preprocessing steps to identify infeasible arcs in the problem in an attempt to reduce the number of decision variables. For that, we propose a set of conditions, which identifies infeasible arcs with respect to time and energy constraints. We also benefit from the station dominance rules presented in Bruglieri et al. (2016).

Throughout this section, h_{ij} denotes either the least possible energy consumption or the highest regenerative braking for arc (i,j) based on the sign of required tractive power for that arc, which depends on the load that is being carried. Hence, to calculate h_{ij}, we assume a load which results in the minimum energy consumption or the highest regenerative braking depending on the resulted tractive power for arc (i,j). Note that in our model, the flow variable x_{ij} is equal to 1 if the vehicle travels from customer/depot i to customer/depot j; and 0 otherwise. Additionally, the binary variable z_{ijs} is used to determine whether the trip from i to j is direct ($z_{ijs} = 0$) or occurs via a station visited on the way ($z_{ijs} = 1$). Note that $\sum_{s\in F} z_{ijs} \leq x_{ij}$, where F represents the set of available stations. We also use the set F_0 that includes the stations and the depot. The conditions proposed in the following determine whether a trip from node i to node j is feasible either directly or via a station. If the conditions are not satisfied, arc (i,j) is deemed infeasible, and we set $x_{ij} = 0$, which also enforces $z_{ijs} = 0$ for all the stations. To assess the feasibility of the arcs, we analyze the trips from the depot to a customer, from a customer to another, and from a customer to the depot.

2.3.1. Depot-to-customer trips

A vehicle departing from the depot, node 0, can visit customer i if it can reach a station or go back to the depot after its visit without violating battery capacity and time-window restrictions. For the accessibility of customer i from the depot there are two possible cases: (a) the vehicle travels directly to customer i; (b) the vehicle travels to customer i after having its battery recharged en route.

In case (a), we define θ_{0i} and $\theta_{i\bar{s}}$ as the earliest times that the vehicle can start serving customer $i \in V$ and arrive at a station or the depot, respectively, where $\bar{s} \in F_{n+1}$.

$$h_{0i} + h_{i\bar{s}} \leq Q \tag{27}$$

$$\theta_{0i} = e_0 + t_{0i} \leq l_i \tag{28}$$

$$\theta_{i\bar{s}} = \max\{\theta_{0i}, e_i\} + s_i + t_{i\bar{s}} \leq l_{\bar{s}} \tag{29}$$

Conditions (27) and (28) impose energy consumption and time-window restrictions on the vehicle to reach customer i after its departure from the depot. Condition (29) checks the time-window feasibility at node $\bar{s} \in F_{n+1}$. Conditions (27)–(29) are checked for each $\bar{s} \in F_{n+1}$, and if at least one $\bar{s} \in F_{n+1}$ can be found satisfying all conditions, the arc $(0,i)$ remains, otherwise the vehicle cannot travel directly from the depot to customer i, thus the next case is considered.

Let us now look into case (b) and define θ_{0s}, θ_{si}, and $\theta'_{i\bar{s}}$ as the earliest times that the vehicle can start recharging at a station $s \in F$, start serving customer $i \in V$, and arrive at $\bar{s} \in F_{n+1}$, respectively. μ_s denotes

the minimum amount of energy that the vehicle should recharge at station $s \in F$ in order to continue its route to reach node $\overline{s} \in F_{n+1}$ after visiting customer i, and is calculated as $\mu_s = h_{si} + h_{i\overline{s}} - (Q - h_{0s})$.

$$h_{0s} \leq Q \tag{30}$$

$$\theta_{0s} = e_0 + t_{0s} \leq l_s \tag{31}$$

$$\theta_{si} = \max\{\theta_{0s}, e_s\} + r(\mu_s) + t_{si} \leq l_i \tag{32}$$

$$h_{si} + h_{i\overline{s}} \leq Q \tag{33}$$

$$\theta'_{i\overline{s}} = \max\{\theta_{si}, e_i\} + s_i + t_{i\overline{s}} \leq l_{\overline{s}} \tag{34}$$

Conditions (30) and (31) impose energy consumption and time window restrictions for the vehicle to reach station s after departing from the depot. Condition (32) checks the time-window feasibility of customer i. Conditions (33) and (34) ensure that the vehicle can arrive at node $\overline{s}$ after visiting customer i without running out of energy or violating the time windows, respectively. These conditions check whether there is a station s that can be visited before reaching at customer i. If (30)–(34) are satisfied for at least one $s \in F$ and one $\overline{s} \in F_{n+1}$, then visiting s en route is feasible; otherwise, z_{0is} is set to zero. If no stations can be found, then the vehicle departing from the depot cannot reach customer i after having been recharged en route.

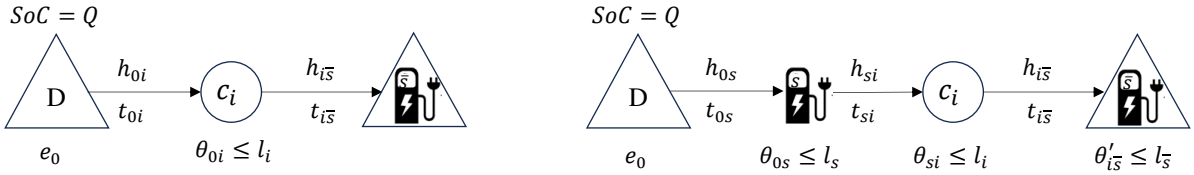

(a) Traveling directly from depot to customer i (b) Traveling from depot to customer i via station s

Figure 2. Conditions for the connectivity of the depot to customer i.

After checking the conditions outlined within cases (a) and (b), arc $(0, i)$ can be removed from the set of potential arcs in the network if the vehicle cannot travel to customer i directly, or via a station from the depot. Both cases are shown in Figure 2, where the last node is represented by a station icon within a triangle, showing that it can be a station or the depot.

2.3.2. Customer-to-customer trips

Customer j is accessible from customer i if the vehicle can reach a station or the depot, $\underline{s} \in F_{n+1}$, after visiting j without violating battery capacity and time window constraints. The highest possible energy in the battery at customer i can be attained if the vehicle travels to i from the depot, a station or any customer except nodes i, j and $n+1$, i.e., $\overline{s} \in N \setminus \{i, j, n+1\}$, where it leaves with a full battery. Thus, the trip is assumed to start at a node $\overline{s} \in N \setminus \{i, j, n+1\}$. In the following, we consider two possible cases: (a) the

vehicle travels directly to customer j; (b) the vehicle travels to customer j after having its battery recharged en route. Case (a) is feasible if all of the following conditions hold for at least one $\overline{s} \in N \setminus \{i, j, n+1\}$ and one $\underline{s} \in F_{n+1}$:

$$\theta_{\overline{s}i} = e_{\overline{s}} + t_{\overline{s}i} \leq l_i \tag{35}$$

$$\theta_{ij} = \max\{\theta_{\overline{s}i}, e_i\} + s_i + t_{ij} \leq l_j \tag{36}$$

$$\theta_{j\underline{s}} = \max\{\theta_{ij}, e_j\} + s_j + t_{j\underline{s}} \leq l_{\underline{s}} \tag{37}$$

$$h_{\overline{s}i} + h_{ij} + h_{j\underline{s}} \leq Q \tag{38}$$

Conditions (35), (36), and (37) ensure time window feasibility for customers i and j, and node $\underline{s} \in F_{n+1}$, respectively. Condition (38) checks whether the battery capacity of the EV is sufficient to complete the trip. If condition (38) does not hold, the vehicle cannot complete this trip without recharging between customer i and customer j, thus case (b) should be considered with the following conditions:

$$h_{\overline{s}i} + h_{is} \leq Q \tag{39}$$

$$h_{sj} + h_{j\underline{s}} \leq Q \tag{40}$$

$$\theta_{is} = \max\{\theta_{\overline{s}i}, e_i\} + s_i + t_{is} \leq l_s \tag{41}$$

$$\theta_{sj} = \max\{\theta^*_{is}, e_s\} + r(\mu'_s) + t_{sj} \leq l_j \tag{42}$$

$$\theta'_{j\underline{s}} = \max\{\theta_{sj}, e_j\} + s_j + t_{j\underline{s}} \leq l_{\underline{s}} \tag{43}$$

where $\mu'_s = h_{sj} + h_{j\underline{s}} - (Q - h_{\overline{s}i} - h_{is})$ is the minimum energy required by the vehicle to travel the path $i \rightarrow s \rightarrow j$, where $s \in F$ is a station that can be feasibly visited in between. Conditions (39) and (40) check whether the battery has sufficient capacity for the required energy to serve customer i and customer j, respectively. Conditions (41), (42), and (43) ensure the time-window feasibility of station s, customer j, and node $\underline{s} \in F_{n+1}$, respectively. If at least one station s satisfying (39)– (43) can be found, then it is possible travel from customer i to customer j via a station; otherwise, z_{ijs} is equal to 0. After checking both cases, arc (i, j) can be removed from the set of potential arcs in the network if customer i is not directly connected to customer j or via a station. Figure 3 shows the conditions under which customer i is connected to customer j. Since we analyze the journeys that can start at a customer, a station or the depot, the first node is represented by a station icon within a circle and a triangle, standing for the customers, depot, and stations.

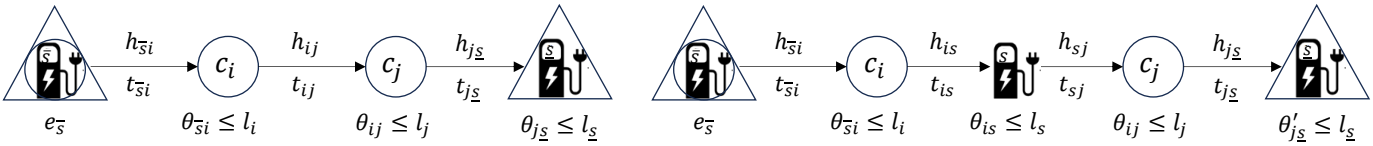

(a) Traveling directly from customer i to j (b) Traveling from customer i to j via station s

Figure 3. Conditions for the connectivity of customer i to customer j.

2.3.3. Customer-to-depot trips

To assess whether the depot, denoted by $n+1$, is accessible from customer j, we use the highest possible energy level when departing from j that is possible if j is visited after the depot, a station or any customer except nodes j and $n+1$, i.e., $\underline{s} \in N \setminus \{j, n+1\}$, from which the vehicle leaves with a full battery. We evaluate if the depot can be reached without violating battery capacity and time window restrictions. Again, the trip from customer j to the depot can be direct (a) or via station (b). For case (a), we consider the following conditions, where $\theta_{\underline{s}j}$ denotes the earliest time when customer j can be served if the vehicle travels from node $\underline{s}$ to customer j, while $\theta_{j,n+1}$ represents the earliest time at which the vehicle can return to the depot after serving customer j:

$$h_{\underline{s}j} + h_{j,n+1} \leq Q \tag{44}$$

$$\theta_{\underline{s}j} = e_{\underline{s}} + t_{\underline{s}j} \leq l_j \tag{45}$$

$$\theta_{j,n+1} = \max\{\theta_{\underline{s}j}, e_j\} + s_j + t_{j,n+1} \leq l_{n+1} \tag{46}$$

Condition (44) checks the driving range feasibility, whereas conditions (45) and (46) control the time-window feasibility of customer j and the depot, respectively, at the end of the trip.

For case (b), let $F_{j,n+1}$ be the set of feasible stations that the vehicle can visit when traveling from customer j to depot $n+1$. The following conditions are considered, where $\mu_s'' = h_{s,n+1} - (Q - h_{\underline{s}j} - h_{js})$ represents the minimum amount of energy the vehicle must recharge at station $s \in F$ to return to the depot and $\theta_{s,n+1}$ represents the earliest time when the vehicle can return to the depot:

$$h_{\underline{s}j} + h_{js} \leq Q \tag{47}$$

$$\theta_{js} = \max\{\theta_{\underline{s}j}, e_j\} + s_j + t_{js} \leq l_s \tag{48}$$

$$h_{s,n+1} \leq Q \tag{49}$$

$$\theta_{s,n+1} = \max\{\theta_{js}, e_s\} + r(\mu_s'') + t_{s,n+1} \leq l_{n+1} \tag{50}$$

Conditions (47) and (48) check the driving range and time-window feasibility of the trip from customer j to station s, respectively, whereas conditions (49) and (50) do the same for the trip from station s to the depot. If there exists at least one station $s \in F$ satisfying (47)–(50), then the depot can be accessed from customer j via a station. Otherwise, $z_{j,n+1,s}$ is equal to 0. After checking the conditions in cases (a) and (b), if customer j is not directly connected to the depot or via a station, arc $(j, n+1)$ can be removed from the set of arcs in the network. Both cases are shown in Figure 4.

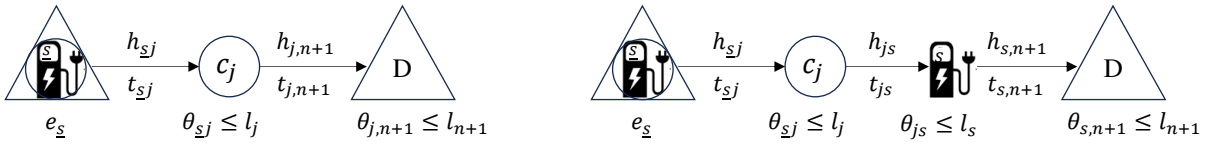

(a) Traveling directly from customer j to the depot (b) Traveling from customer j to the depot via station s

Figure 4. Conditions for the connectivity of customer j to depot n+1

2.4. Valid inequalities

We add the following valid inequalities to tighten the model and speed up the solution process.

$$e_0 + t_{0i} \le \tau_i \le l_{n+1} - t_{i,n+1} \qquad \forall\, i \in N \tag{51}$$

$$x_{ij} - \sum_{s \in F_{i,j}} z_{ijs} = 0 \qquad \forall\, (i,j) \in E \tag{52}$$

The time-window constraints associated with the stations and customers are tightened using inequalities (51). Let E represent the set of subsequent customers i and j that can be served only by recharging the battery at a station in between. Equation (52) ensures that the customers in this set can only be connected through a station from set $F_{i,j}$, which denotes the set of stations that can be feasibly visited between customer i and customer j.

3. Linear formulations for EVRPTW-GR

NL-Model formulates the problem using a general energy consumption function $h_{ij}(M_{ij})$ along arc $(i,j) \in A$, which is nonlinear and cannot be tractable due to conditional nature of $h_{ij}(M_{ij})$. Therefore, we propose three alternative linearizations as MILP formulations. In the first model (MILP1), nonlinearity is mitigated by approximating energy consumption. The second MILP model (MILP2) incorporates additional decision variables and constraints to linearize NL-Model. This model calculates the objective function by summing the energy consumption on each arc traveled. The third model (MILP3) has the same structure with MILP2 but calculates the objective function by tracking the remaining SoC of each EV upon its arrival at depot and the amount of recharged energy at the stations.

3.1. MILP1: Approximate model

The nonlinearity in this model arises from the variability in the sign of the tractive power, conditioned to the combination of the road gradient and the current weight of the vehicle, which makes the problem unsolvable. To address this issue and enable a solution, it is necessary to eliminate conditional statements from the model. To achieve this, we propose defining the necessary tractive power associated with arc $(i,j) \in A$ as a free decision variable, denoted by p_{ij}, as it may take negative or positive values depending

on the topography of that arc as well as the weight of the vehicle while traveling on that arc. Assuming both efficiency values equal to one ($\mu = \mu_r = 1$) unifies equations (6) and (7) by eliminating the conditional statement and transforms the model into a MILP. Note that this approximation underestimates the consumed energy, while overestimating the energy regenerated. In this simplified scenario, the consumption while traveling from node i to node j is denoted by $h_{ij}(M_{ij}) = \tilde{h}_{ij}$. The resulting problem, referred to as MILP1, provides an approximate solution to the original problem, if feasible. $\tilde{h}_{ij}$ is defined as a sign-free variable, as it tracks both the energy consumed and the energy gained through regenerative braking depending on the road topography and the weight of the vehicle, as in the calculation of p_{ij}. In the former case, $\tilde{h}_{ij}$ has a positive value, while it is assigned a negative value in the latter one. MILP1 is formulated as follows:

$$\text{Min} \sum_{(i,j)\in A} \tilde{h}_{ij} \tag{53}$$

subject to (9) – (19), (23) – (26), and

$$\left(M_{ij} - \sum_{s\in F} \widehat{M}_{ijs}\right)\beta_{ij} + \left(x_{ij} - \sum_{s\in F} z_{ijs}\right)\gamma \le p_{ij} \qquad \forall\, i \in V_0, j \in V_{n+1}, i \ne j \tag{54}$$

$$\sum_{\substack{i\in V_0 \\ i\ne j}} \widehat{M}_{ijs}\,\beta_{sj} + \sum_{\substack{i\in V_0 \\ i\ne j}} z_{ijs}\,\gamma \le p_{sj} \qquad \forall j \in V_{n+1}, s \in F \tag{55}$$

$$\sum_{\substack{j\in V_{n+1} \\ j\ne i}} \widehat{M}_{ijs}\,\beta_{is} + \sum_{\substack{j\in V_{n+1} \\ j\ne i}} z_{ijs}\,\gamma \le p_{is} \qquad \forall\, i \in V_0, s \in F \tag{56}$$

$$\frac{p_{ij} d_{ij}}{\overline{V}} \le \tilde{h}_{ij} \qquad \forall\, i \in V'_0, j \in V'_{n+1}, i \ne j \tag{57}$$

$$0 \le y_j \le y_i - \tilde{h}_{ij} + U\left(1 - x_{ij} + \sum_{s\in F} z_{ijs}\right) \qquad \forall\, i \in V_0, j \in V_{n+1}, i \ne j \tag{58}$$

$$0 \le y_{ijs} \le y_i - \tilde{h}_{is} + U(1 - z_{ijs}) \qquad \forall\, i \in V_0, j \in V_{n+1}, s \in F, i \ne j \tag{59}$$

$$y_j \le Y_{ijs} - \tilde{h}_{sj} + U(1 - z_{ijs}) \qquad \forall\, i \in V_0, j \in V_{n+1}, s \in F, i \ne j \tag{60}$$

$$p_{ij} \text{ free} \qquad \forall\, (i,j) \in A \tag{61}$$

$$\tilde{h}_{ij} \text{ free} \qquad \forall\, (i,j) \in A \tag{62}$$

The objective function (53) minimizes the total approximated energy consumption. Constraints (54) – (56) are related to tractive power calculations. If the vehicle travels from node i to j directly, then z_{ijs} and $\widehat{M}_{ijs}$ will be equal to zero, which makes constraints (55) and (56) redundant, and constraints (54) become active in the tractive power calculation. If a station s is visited in between, then $\widehat{M}_{ijs}$ and M_{ij} will be equal, which makes constraints (54) redundant. In this case, the tractive power needed from node i to station s and from station s to node j are calculated by constraints (55) and (56), respectively. Constraints (57) approximate

the energy consumption on arc $(i,j) \in A$ under the assumption that efficiency values are all equal to one. Constraints (58) – (60) are similar to (20) – (22), but instead of using the energy consumption function, $h_{ij}(M_{ij})$, a decision variable, $\tilde{h}_{ij}$ that approximates the energy consumption is used, where $U = Q + max_{(i,j)\in A}(\tilde{h}_{ij})$. Finally, constraints (61) and (62) define the domain of the decision variables.

3.2. MILP2: Consumption-based objective

MILP1 is an approximate model; thus, its solution can be infeasible to the original problem when the real efficiency values are used in calculating the energy consumption. Therefore, we propose a linearized version of NL-Model by employing additional decision variables and constraints. The energy consumption along arc $(i,j) \in A$, denoted by h_{ij}, is calculated by either Equations (6) or (7) depending on the sign of the tractive power, p_{ij}, which is also determined by the road gradient as well as the current weight of the vehicle. p_{ij} tracks the required tractive power in kW per unit distance for arc $(i,j) \in A$. To handle the nonlinearity due to the relationship between h_{ij} and p_{ij}, an additional binary decision variable, o_{ij} is introduced, which takes value 1 if p_{ij} is positive and 0 otherwise. MILP2 is formulated as follows:

$$\text{Min} \sum_{(i,j)\in A} h_{ij} \tag{63}$$

subject to (9) – (19), (23) – (26), (54) – (56), (61), and

$$Q(o_{ij} - 1) \le p_{ij} \le Q o_{ij} \qquad \forall\, i \in V'_0, j \in V'_{n+1}, i \ne j \tag{64}$$

$$\frac{p_{ij} d_{ij}}{\overline{V}.\mu} + Q(o_{ij} - 1) \le h_{ij} \qquad \forall\, i \in V'_0, j \in V'_{n+1}, i \ne j \tag{65}$$

$$\frac{\mu_r . p_{ij} d_{ij}}{\overline{V}} - Q o_{ij} \le h_{ij} \qquad \forall\, i \in V'_0, j \in V'_{n+1}, i \ne j \tag{66}$$

$$0 \le y_j \le y_i - h_{ij} + U\left(1 - x_{ij} + \sum_{s\in F} z_{ijs}\right) \qquad \forall\, i \in V_0, j \in V_{n+1}, i \ne j \tag{67}$$

$$0 \le y_{ijs} \le y_i - h_{is} + U(1 - z_{ijs}) \qquad \forall\, i \in V_0, j \in V_{n+1}, s \in F, i \ne j \tag{68}$$

$$y_j \le Y_{ijs} - h_{sj} + U(1 - z_{ijs}) \qquad \forall\, i \in V_0, j \in V_{n+1}, s \in F, i \ne j \tag{69}$$

$$o_{ij} \in \{0,1\}, h_{ij} \text{ free} \qquad \forall\, (i,j) \in A \tag{70}$$

The objective function (63) minimizes the total energy consumption by summing the energy consumption along the arcs traveled by EVs. Constraints (64) connect variables o_{ij} and p_{ij}, ensuring that o_{ij} takes value one if the tractive power needed to travel on arc (i,j) is positive, and it is forced to be zero if the tractive power is negative. Then, the value of o_{ij} determines if constraints (65) or (66) are used to calculate the energy consumption for arc (i,j). If the required tractive power is positive and therefore $o_{ij} = 1$, constraints

(65) are active, calculating the consumed energy along arc (i,j). If the required tractive power is negative and therefore $o_{ij} = 0$, constraints (66) are active, and they calculate the energy gained by regenerative braking while traveling along arc (i,j). Constraints (67) – (69) mirror constraints (58) – (60), substituting the energy consumption approximation, $\tilde{h}_{ij}$, with the actual energy consumption, h_{ij}. Constraints (70) illustrate the domain for decision variables.

3.3. MILP3: SoC-based objective

An alternative to MILP2 is presented where the objective function calculates the total energy consumption by tracking the remaining SoC of each EV upon arrival to depot and the amount of recharged energy at the stations. Dummy departure and arrival depots associated with each tour are used to track the SoC of the EVs upon arrival at their respective depot node. The sets of departure and arrival depots are denoted as DD and AD, respectively. Given the utilization of dummy departure and arrival depots, the sets employed in this formulation are presented in Table 3.

Table 3. Updated sets for MILP3

DD	Set of dummy departure depots
AD	Set of dummy arrival depots
V_0	Set of customers and dummy departure depots; $V_0 = \{V \cup DD\}$
V_{n+1}	Set of customers and dummy arrival depots; $V_{n+1} = \{V \cup AD\}$
V'_0	Set of customers, stations, and dummy departure depots; $V'_0 = \{V \cup F \cup DD\}$
V'_{n+1}	Set of customers, stations, and dummy arrival depots; $V'_0 = \{V \cup F \cup AD\}$
$V_{0,n+1}$	Set of customers and dummy departure and arrival depots $V_{0,n+1} = \{V \cup DD \cup AD\}$

MILP3 is formulated as follows:

$$\text{Min} \left(\sum_{i \in DD} y_i - \sum_{i \in AD} y_i \right) + \sum_{i \in V_0} \sum_{j \in V_{n+1}} \sum_{s \in F} (Y_{ijs} - y_{ijs}) \tag{71}$$

subject to (9) – (19), (23) – (26), (54) – (56), (61), (64) – (70)

In this formulation, the objective function (71) aims at minimizing the energy consumption across all routes associated with each dummy depot. The first component presents the difference between the remaining energy levels of a vehicle's SoC upon reaching the arrival depot at the end of its journey and the initial SoC when departing from the depot. The second component aggregates the energy replenished at the stations visited along the routes.

Throughout the remainder of this paper, we will investigate the performance of the proposed mathematical formulations by analyzing the results obtained by solving the corresponding models using the data generated for this problem.

4. Data generation and computational experiments

As no benchmark data exist for this problem in the literature, we generate dataset based on well-known Schneider et al. (2014) instances for the EVRPTW to perform the computational tests for small-size instances. In line with Rastani et al. (2021), we address realistic considerations regarding vehicle cargo capacity and customer demands by assuming an electric truck based on the specifications provided by Demir et al. (2012). Given the truck's capacity of 3650 kg, demand quantities are standardized to appropriate weights through multiplication by the ratio (3650/original capacity). We set the efficiency factor that is used when the tractive power is positive (μ) to be 0.81, reflecting the superior efficiency of EVs compared to ICEVs. Additionally, the energy factor when the tractive power is negative, including regenerative braking efficiency (μ_r) is assumed to be 0.8, indicating that 80% of the energy regenerated during braking could be stored in the battery (Asamer et al., 2016; Lowell, 2020). Furthermore, given the assumption in the original data that EVs consume one unit of energy per unit distance/time traveled, we make a conversion in the energy consumption calculations to be able to utilize the benchmark data. Basically, by using the curb weight of the vehicle we compute the actual energy consumption per unit distance on a flat network using Equation (4) and scale it to one $(h_{ij} = 1)$. This way, we standardize the energy consumption by dividing the actual energy consumption by the energy consumption of an empty vehicle traveling one unit of distance on a flat network. We assume that the vehicles move at a constant speed disregarding vehicle acceleration. The instances are solved using Gurobi 10.0 with a 2-hour time limit in Python 3.8 and all runs are performed on an Intel Core (TM) i7-8700 processor with 3.20 GHz speed and 32 GB RAM.

4.1. Data generation

In this study, we create a dataset that incorporates road gradient information, which provides a more comprehensive understanding of transportation dynamics, enabling deeper insights into energy consumption patterns and route optimization strategies. By integrating this previously overlooked factor, our dataset offers researchers and practitioners an invaluable resource for developing more accurate and effective transportation models and solutions.

To generate road gradients for the arcs on the network, we consistently assign altitudes to all nodes in the benchmark instance. The widely recognized *k*-means clustering algorithm is employed to cluster the nodes in the data based on distance criterion. Each cluster captures a topographical feature such as a hill or valley reflecting those found within an urban area. After the clusters are formed, a high or a low altitude is allocated to the center of each cluster. Subsequently, the altitude of the individual nodes in each cluster is adjusted based on their distances from the respective cluster center.

The EVRPTW dataset from Schneider et al. (2014) comprises 36 small-size instances with 5, 10, and 15

customers, and 56 large-size instances with 100 customers, which are generated based on Solomon's (1987) VRPTW instances. The instances are categorized by the geographic distribution of customers: clustered (c-type), random (r-type), and a combination of clustered and random (rc-type). Additionally, type-1 problems (subsets r1, c1, rc1) feature a short planning horizon with narrow customer time windows, whereas type-2 problems (subsets r2, c2, rc2) have a long planning horizon with wider time windows. We form two, three, four, and ten clusters in the instances with 5, 10, 15, and 100 customers, respectively. Using large-size instances, we also create medium-size instances by randomly selecting 25 and 50 customers and keeping the stations as in the original data. Regarding the road gradients, three levels are considered based on established road gradient standards: *Level*, *Nearly Level*, and *Very Gentle Slope*. In the *Level* case, the network is predominantly flat, with zero average absolute road gradients. For the *Nearly Level* and *Very Gentle Slope* cases, the average absolute road gradients fall within the ranges of [0.5,2) and [2,5) percent, respectively, as defined in geographical fieldwork standards (Geography Fieldwork, 2024). These gradients are considered relatively mild. For high-speed motorways, the recommended maximum gradient is 3%, while for all-purpose single-carriageway roads, the desirable maximum gradient is 6%. Consequently, road networks with these characteristics are classified as having moderate gradients (GCELAB, 2020). An example topography and the nodes are illustrated in Figure 5. In this figure, depot, customer nodes, and stations are represented by a triangle, circles, and squares, respectively. Additionally, a color bar has been incorporated to represent node altitudes, aiding in the visualization of terrain variations along the network. This network is clustered, and each node is assigned an altitude determined by its proximity to the respective cluster center.

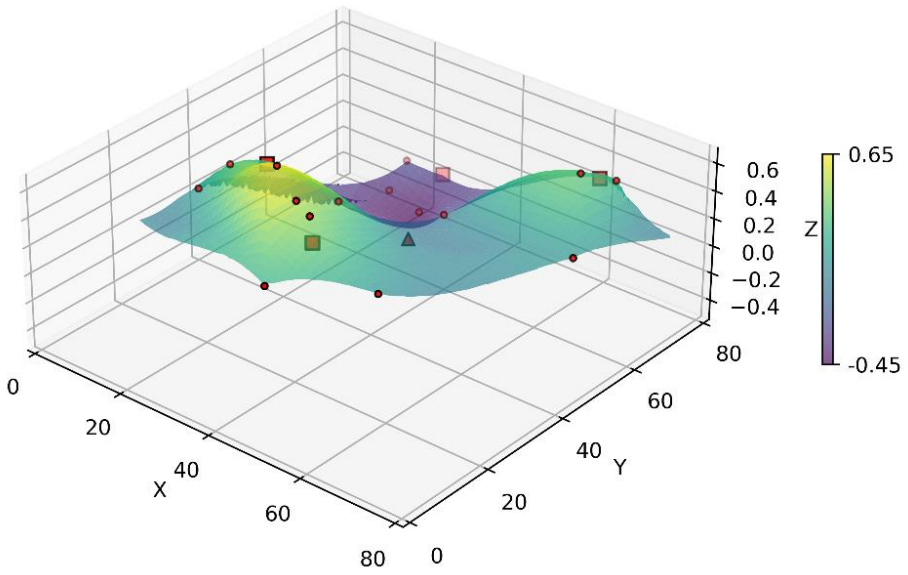

Figure 5. Topography and geographical locations of nodes in an instance (c103c15-s5).

4.2. Performance analysis of linear formulations

We first analyze the performance of the proposed models presented in Section 2. NL-Model is a nonlinear model that is not directly solvable. Therefore, we present results by solving proposed linearized models using the instances described in Section 4.1 under the *Nearly Level* topography scenario. The comparative results are presented in Table 4 and Table 5 for small- and medium-size instances, respectively, where "*#Veh*", "*EC*", "*t*(*sec*)", and "*%Gap*" denote fleet size, energy consumption, the computational time in seconds, and percentage optimality gap that Gurobi reports at the end of time limit, respectively. Column "Instance" indicates the name of the instances, which includes the information related to the number of customers and stations. For example, "r209c15-s5" is an instance with 15 customers and five stations. The "Avg." rows display the mean values for fleet size, energy consumption, run time, and optimality gap across 5-, 10-, and 15-customer instances in Table 4, and 25- and 50-customer instance in Table 5. The overall averages for all instances are summarized in the "Total Avg." row.

Due to the hierarchical nature of the objective function, where minimizing the number of vehicles is the primary objective and minimizing total energy consumption is the secondary, the reported results correspond to the smallest fleet size for which Gurobi was able to find a feasible solution, if any. For the small-size instances presented in Table 4, MILP2 successfully solves 35 out of 36 instances optimally, providing an upper bound within the two-hour time limit for one instance (rc204c15). MILP1, which approximates NL-Model by ignoring efficiency factors, also solves 35 instances. However, to analyze the obtained solutions, they are mapped to calculate actual energy consumptions using real-world efficiency values by replacing the approximated values. In 29 out of 36 instances, the solutions (routes) are identical to those obtained by solving MILP2, and therefore the mapped objective function values are also the same. However, in four out of the remaining seven instances, where the solutions (routes) differ from those of MILP2, the solutions are found to be infeasible for the original problem subject to real efficiency values, as indicated by "INF" in Table 4. In the other two instances, which are shown in bold, the mapped objective functions are worse than those of MILP2. Finally, for "rc204c15", the optimality is not proved within a two-hour time limit, and the reported solution at the end of the time limit is again worse than that achieved by MILP2. The results obtained using MILP1 demonstrate that ignoring efficiency factors may lead to worse and potentially infeasible routes when real-world conditions are applied. However, they also show that MILP1 is about 55% faster than MILP2, excluding the computational time for rc204c15 that hits the two-hour limit for both models. The results obtained using MILP3 are consistent with those of MILP2, but overall, MILP3 is approximately 91% slower. This difference arises from how the objective function is formulated: In MILP3, the objective function (71) minimizes energy consumption by calculating the exact battery SoC values for the EVs upon their arrival at and departure from stations. On the other hand, the

objective function of MILP2 (63) minimizes energy consumption by considering only the energy over the traveled arcs, without calculating the exact SoC values at the stations but instead focusing on the difference in SoC values, thereby simplifying the problem and making it easier to solve. In 34 out of 36 instances, MILP2 and MILP3 yield identical solutions. In the remaining two instances, the upper bounds obtained within the two-hour limit are worse than those of MILP2, which aligns with the inferior performance of MILP3 in terms of computational time.

Table 4. Comparison of results obtained for *Nearly Level* topography for small-size instances.

	MILP1				MILP2			MILP3		
Instance	*#Veh*	*EC*	*t (sec)*	*%Gap*	*EC*	*t (sec)*	*%Gap*	*EC*	*t (sec)*	*%Gap*
r104c5-s3	2	142.97	<1	0.00	142.97	<1	0.00	142.97	<1	0.00
r105c5-s3	2	184.89	<1	0.00	184.89	<1	0.00	184.89	<1	0.00
r202c5-s3	1	143.18	<1	0.00	143.18	<1	0.00	143.18	<1	0.00
r203c5-s4	1	211.32	<1	0.00	211.32	<1	0.00	211.32	<1	0.00
c101c5-s3	2	292.15	<1	0.00	292.15	<1	0.00	292.15	<1	0.00
c103c5-s2	1	196.20	<1	0.00	196.20	<1	0.00	196.20	<1	0.00
c206c5-s4	1	263.37	<1	0.00	263.37	<1	0.00	263.37	<1	0.00
c208c5-s3	1	186.15	<1	0.00	186.15	<1	0.00	186.15	<1	0.00
rc105c5-s4	2	250.51	<1	0.00	250.51	<1	0.00	250.51	<1	0.00
rc108c5-s4	2	258.27	<1	0.00	258.27	<1	0.00	258.27	<1	0.00
rc204c5-s4	1	187.74	<1	0.00	187.74	<1	0.00	187.74	1	0.00
rc208c5-s3	1	188.34	<1	0.00	188.34	<1	0.00	188.34	<1	0.00
Avg.	1.42	208.76	0.10	0.00	208.76	0.16	0.00	208.76	0.25	0.00
r102c10-s4	3	302.22	1	0.00	302.22	2	0.00	302.22	9	0.00
r103c10-s3	2	INF	9	0.00	223.01	32	0.00	223.01	240	0.00
r201c10-s4	1	311.85	1	0.00	311.85	3	0.00	311.85	2	0.00
r203c10-s5	2	259.03	3	0.00	259.03	11	0.00	259.03	7200	90.07
c101c10-s5	3	INF	<1	0.00	433.68	1	0.00	433.68	119	0.00
c104c10-s4	2	324.79	9	0.00	324.79	22	0.00	324.79	7200	98.93
c202c10-s5	1	335.05	<1	0.00	335.05	1	0.00	335.05	1	0.00
c205c10-s3	2	270.04	<1	0.00	270.04	1	0.00	270.04	58	0.00
rc102c10-s4	5	465.50	<1	0.00	465.50	1	0.00	465.50	7200	34.67
rc108c10-s4	3	374.59	1	0.00	374.59	3	0.00	374.59	115	0.00
rc201c10-s4	1	437.09	<1	0.00	437.09	<1	0.00	437.09	<1	0.00
rc205c10-s4	2	380.39	1	0.00	380.39	1	0.00	380.39	25	0.00
Avg.	2.25	346.06	2.31	0.00	343.10	6.53	0.00	343.10	1847	18.64
r102c15-s8	5	418.58	5	0.00	418.58	17	0.00	418.58	7200	99.99
r105c15-s6	4	403.60	2	0.00	403.60	5	0.00	403.60	7200	55.10
r202c15-s6	2	406.51	42	0.00	406.51	142	0.00	408.33	7200	98.92
r209c15-s5	1	INF	145	0.00	355.35	350	0.00	355.35	7200	88.07
c103c15-s5	3	INF	90	0.00	400.90	260	0.00	400.90	7200	99.99
c106c15-s3	3	311.09	3	0.00	311.09	7	0.00	311.09	7200	99.99
c202c15-s5	2	449.40	68	0.00	449.40	282	0.00	449.40	7200	99.99
c208c15-s4	2	415.93	51	0.00	415.93	112	0.00	415.93	7200	90.43
rc103c15-s5	4	**447.33**	61	0.00	447.12	147	0.00	447.12	7200	99.99
rc108c15-s5	3	434.81	397	0.00	434.81	716	0.00	434.81	7200	99.99
rc202c15-s5	2	**419.15**	3	0.00	416.91	6	0.00	416.91	7200	98.70
rc204c15-s7	1	430.10	7200	23.70	426.42	7200	28.75	443.27	7200	99.99
Avg.	2.67	413.65	672	1.98	407.22	770	2.40	408.77	7200	94.26
Total Avg.	2.11	322.82	225	0.66	319.69	259	0.80	320.21	3016	37.63

Table 5 presents the results for medium-size instances, including 25- and 50-customer problems with 21 charging stations within four-hour time limit. For smaller instances, the models can typically determine the minimum required number of EVs. However, in medium-size instances, the reported number of EVs may not always be optimal; rather, the solutions correspond to the best feasible ones found within the time limit and may not represent the global optimum. For example, in instances "c102c25-s21" and "c102c50-s21", MILP1 provides feasible solutions with one and two fewer EVs in comparison to MILP2. This shows the increasing computational difficulty and intractability as problem size grows. On the other hand, because MILP1 is an approximation of the original problem, its solutions may be infeasible when mapped back to the full problem. This occurred in eight of the twelve 25-customer instances and three of the four 50-customer instances. Among the three instances where MILP1 returned feasible solutions using the same number of EVs as MILP2, MILP1 outperformed MILP2 in "rc104c25-s21" but performed worse in "rc103c25-s21" and "rc106c25-s21" within the same time limit. Meanwhile, MILP3 exhibited a significant drop in performance on medium-size instances, requiring on average 27% and 31% more EVs for the 25- and 50-customer instances, respectively.

Table 5. Comparison of results obtained for *Nearly Level* topography for medium-size instances.

	MILP1				MILP2				MILP3			
Instance	*#Veh*	*EC*	*t (sec)*	*%Gap*	*#Veh*	*EC*	*t (sec)*	*%Gap*	*#Veh*	*EC*	*t (sec)*	*%Gap*
c101c25-s21	5	INF	41	0.00	5	770.18	166	0.00	7	700.21	14400	100.00
c102c25-s21	5	600.26	4614	0.00	6	605.45	14400	1.68	6	666.94	14400	100.00
c104c25-s21	4	INF	14400	9.64	4	449.77	14400	11.34	7	691.92	14400	100.00
c108c25-s21	4	INF	4087	0.00	4	506.52	14400	6.67	5	517.59	14400	100.00
r102c25-s21	8	INF	667	0.00	8	616.65	3334	0.00	8	628.25	14400	100.00
r104c25-s21	5	INF	3622	0.00	5	428.77	14400	6.16	8	532.38	14400	100.00
r107c25-s21	6	INF	3461	0.00	6	527.08	14400	4.64	7	609.73	14400	100.00
r110c25-s21	5	INF	14400	1.85	6	494.58	14400	8.27	8	567.96	14400	100.00
rc101c25-s21	6	INF	28	0.00	7	730.83	97	0.00	7	730.83	14400	94.23
rc103c25-s21	6	615.06	14400	7.34	6	614.53	14400	9.29	9	742.06	14400	100.00
rc104c25-s21	7	642.44	14400	13.05	7	647.25	14400	15.61	9	759.13	14400	100.00
rc106c25-s21	6	645.11	161	0.00	6	644.74	1326	0.00	8	687.09	14400	100.00
Avg.	5.58	625.72	6190	2.66	5.83	586.36	10010	5.30	7.42	652.84	14400	99.52
c101c50-s21	9	INF	2742	0.00	9	933.10	14400	3.63	15	1292.71	14400	100.00
c102c50-s21	12	864.46	14400	12.31	14	911.60	14400	12.01	18	1253.74	14400	100.00
r102c50-s21	13	INF	14400	10.23	16	1059.59	14400	7.92	21	1450.28	14400	100.00
r107c50-s21	12	INF	14400	18.39	16	994.42	14400	18.31	18	1224.97	14400	100.00
Avg.	11.50	864.46	11485	10.23	13.75	974.68	14400	10.47	18.00	1305.42	14400	100.00

Table 4 and Table 5 show that MILP2 yields more accurate solutions compared than MILP1 and runs faster than MILP3. For further evaluation, we benchmark MILP2 against the load-dependent model of Rastani and Çatay (2023) using the small-size dataset. Specifically, we set all gradients to zero, reducing the

problem to the Load-Dependent EVRPTW. The results obtained within a two-hour time limit are presented in Table 6.

Table 6. Performance evaluation of MILP2 using Load-Dependent EVRPTW data.

	Rastani & Çatay (2023)				MILP2			
Instance	*#Veh*	*EC*	*t(sec)*	*%Gap*	*#Veh*	*EC*	*t(sec)*	*%Gap*
r104c5-s3	2	141.54	<1	0.00	2	141.54	<1	0.00
r105c5-s3	2	159.23	<1	0.00	2	159.23	<1	0.00
r202c5-s3	1	144.12	<1	0.00	1	144.12	<1	0.00
r203c5-s4	1	181.32	<1	0.00	1	181.32	<1	0.00
c101c5-s3	2	266.02	<1	0.00	2	266.02	<1	0.00
c103c5-s2	1	186.83	<1	0.00	1	186.83	<1	0.00
c206c5-s4	1	250.63	<1	0.00	1	250.63	<1	0.00
c208c5-s3	1	168.91	<1	0.00	1	168.91	<1	0.00
rc105c5-s4	2	256.62	<1	0.00	2	256.62	<1	0.00
rc108c5-s4	2	264.00	<1	0.00	2	264.00	<1	0.00
rc204c5-s4	1	188.58	<1	0.00	1	188.58	<1	0.00
rc208c5-s3	1	170.82	<1	0.00	1	170.82	<1	0.00
Avg	1.42	198.22	0.25	0.00	1.42	198.22	0.22	0.00
r102c10-s4	3	336.00	4	0.00	3	336.00	9	0.00
r103c10-s3	2	220.50	213	0.00	2	220.50	53	0.00
r201c10-s4	1	262.40	4	0.00	1	262.40	2	0.00
r203c10-s5	1	227.26	3297	0.00	1	227.26	11	0.00
c101c10-s5	3	410.10	11	0.00	3	410.10	<1	0.00
c104c10-s4	2	305.64	7200	94.17	2	305.64	14	0.00
c202c10-s5	1	319.04	<1	0.00	1	319.04	2	0.00
c205c10-s3	2	233.74	18	0.00	2	233.74	<1	0.00
rc102c10-s4	5	475.00	54	0.00	5	475.00	1	0.00
rc108c10-s4	3	364.62	46	0.00	3	364.62	9	0.00
rc201c10-s4	1	424.49	<1	0.00	1	424.49	<1	0.00
rc205c10-s4	2	334.54	103	0.00	2	334.54	2	0.00
Avg	2.17	326.11	913	7.85	2.17	326.11	8.77	0.00
r102c15-s8	5	430.83	7200	66.37	5	430.83	26	0.00
r105c15-s6	4	350.09	7200	47.08	4	350.09	2	0.00
r202c15-s6	2	365.06	7200	99.99	2	365.06	53	0.00
r209c15-s5	1	347.31	7200	91.13	1	347.31	1549	0.00
c103c15-s5	3	403.18	7200	89.78	3	401.97	2272	0.00
c106c15-s3	3	352.29	2478	0.00	3	352.29	67	0.00
c202c15-s5	2	393.19	7200	99.32	2	393.19	291	0.00
c208c15-s4	2	310.12	7200	41.46	2	310.12	5	0.00
rc103c15-s5	4	415.79	7200	85.32	4	415.79	108	0.00
rc108c15-s5	4	430.69	7200	99.99	4	417.92	947	0.00
rc202c15-s5	2	403.03	7200	34.72	2	403.03	18	0.00
rc204c15-s7	1	402.41	7200	100.00	1	411.92	7200	29.42
Avg	2.75	383.67	6807	71.26	2.75	383.29	1045	2.45
Overall Avg	2.11	302.67	2573	26.37	2.11	302.54	351	0.82

The results indicate that MILP2 outperforms the model proposed by Rastani and Çatay (2023). Specifically, MILP2 yields optimal solutions for 35 out of 36 benchmark instances and provides improved solutions for "c103c15-s5" and "rc108c15-s5." Additionally, MILP2 solves the load-dependent problem approximately 86% faster. This improvement can be attributed to its model formulation, as well as the incorporation of variable reduction techniques and valid inequalities. Based on the results in Tables 4-6, MILP2 is selected for subsequent analyses.

4.3. Effect of road gradient and regenerative braking on route planning

In this section, we analyze how considering the topography of the network affects the solutions from total energy consumption and route planning points of view. For this analysis, we compare the results obtained using MILP2 for the *Level*, *Nearly Level*, and *Very Gentle Slope* cases. The *Level* scenario represents a flat network and corresponds to the load-dependent case, where the energy consumption is affected only by the cargo load (Rastani et al., 2021), thus constituting a reference case in this analysis. In contrast, the *Nearly Level* and *Very Gentle Slope* scenarios account for road gradients in addition to cargo load. The solutions for these different scenarios are summarized in Table 7, where "*Dist*" indicates the total distance traveled in each solution, and "*%Reg*" shows energy gained through regenerative braking as percentage of battery capacity. "*%ΔEC*" represents the percentage variation in energy consumption by comparing the *Nearly Level* and *Very Gentle Slope* cases to the *Level* case, when the fleets consist of the same number of vehicles in both cases.

The results indicate that in the *Nearly Level* case, the number of vehicles increases by one in two instances (highlighted in bold) compared to the *Level* case. Additionally, while energy consumption values are generally higher (5.9% on average), there are nine instances where energy consumption decreases. This reduction can be attributed to the EVs conserving energy through regenerative braking. Additionally, accounting for road gradients allows an EV not fully recharge its battery at the depot overnight and reduce energy cost if it encounters downhill road segments upon its departure, providing the opportunity to regenerate energy through braking. Note that in the case where the vehicle travels on downhill roads upon departure from depot, energy savings can be higher in a delivery problem involving heavy goods as a loaded EV moving downhill can regenerate more energy. In five instances, EVs do not require to be charged fully overnight, and for those instances on average they start their tour from depot with 96.7% SoC. The most substantial energy savings are observed in "c106c15-s3" with an 11.7% reduction in energy consumption compared to the *Level* case. On the other hand, the highest increase in energy consumption occurs in "c208c15-s4", with a 34.1% rise.

In the *Very Gentle Slope* case, as the average absolute road gradient is increased, the results indicate that the number of vehicles increases by one in six instances (highlighted in bold) compared to the *Level* case. Furthermore, 12 instances out of 36 become infeasible even when a dedicated vehicle is dispatched to each customer. Although in this case the increase in energy consumption compared to the *Level* case is more intense, 16.2% on average, there are still two instances, where savings in energy consumption are observed compared to the *Level* case. On average, across eight instances, EVs depart from the depot with 89.7% SoC, resulting in savings on overnight charging attributed to regenerative braking.

Table 7. Results for different topographies.

Instance	Level			Nearly Level					Very Gentle Slope				
	#Veh	*EC*	*Dist*	*#Veh*	*EC*	*Dist*	*%Reg*	*%ΔEC*	*#Veh*	*EC*	*Dist*	*%Reg*	*%ΔEC*
r104c5-s3	2	141.54	136.69	2	142.97	140.26	2.61	1.01	–	INF			–
r105c5-s3	2	159.23	156.08	2	184.89	181.20	6.45	16.12	2	192.68	181.88	31.23	21.01
r202c5-s3	1	144.12	142.65	1	143.18	141.29	0.94	-0.65	1	200.18	191.47	21.03	38.90
r203c5-s4	1	181.32	179.06	1	211.32	205.45	11.76	16.55	1	220.41	211.00	22.40	21.56
c101c5-s3	2	266.02	257.75	2	292.15	278.76	8.96	9.82	–	INF			–
c103c5-s2	1	186.83	175.37	1	196.20	184.50	2.73	5.02	**2**	192.80	185.01	11.80	–
c206c5-s4	1	250.63	245.34	1	263.37	258.58	0.00	5.08	1	373.47	367.74	0.00	49.01
c208c5-s3	1	168.91	164.34	1	186.15	180.95	1.24	10.20	–	INF			–
rc105c5-s4	2	256.62	241.30	2	250.51	235.07	8.15	-2.38	2	257.81	238.27	24.68	0.46
rc108c5-s4	2	264.00	253.93	2	258.27	249.94	0.58	-2.17	–	INF			–
rc204c5-s4	1	188.59	185.16	1	187.74	184.13	0.00	-0.45	1	189.58	182.61	9.07	0.52
rc208c5-s3	1	170.82	167.98	1	188.34	186.41	0.47	10.25	–	INF			–
Avg.	1.42	198.22	192.14	1.42	208.76	202.21	3.66	5.70	1.43	232.42	222.57	17.17	21.91
r102c10-s4	3	336.00	321.42	3	302.22	287.83	9.64	-10.05	3	328.32	306.69	29.48	-2.29
r103c10-s3	2	220.50	208.99	2	223.01	210.39	7.39	1.14	2	219.40	207.33	6.37	-0.50
r201c10-s4	1	262.40	255.50	1	311.85	298.67	17.33	18.85	**2**	293.37	280.40	29.61	–
r203c10-s5	1	227.26	222.64	**2**	259.03	254.91	2.82	–	–	INF			–
c101c10-s5	3	410.10	388.25	3	433.68	405.72	20.77	5.75	3	466.00	421.28	59.44	13.63
c104c10-s4	2	305.64	284.17	2	324.79	300.21	0.07	6.27	2	343.93	308.94	23.91	12.53
c202c10-s5	1	319.04	304.06	1	335.05	**312.37**	22.16	5.02	1	354.77	**312.37**	71.32	11.20
c205c10-s3	2	233.74	228.28	2	270.04	**256.23**	18.49	15.53	2	279.81	**256.23**	42.83	19.71
rc102c10-s4	5	475.00	460.98	5	465.50	452.35	7.93	-2.00	–	INF			–
rc108c10-s4	3	364.62	347.90	3	374.59	348.82	30.63	2.73	3	423.61	388.14	59.65	16.18
rc201c10-s4	1	424.49	414.81	1	437.09	415.97	28.73	2.97	1	449.98	422.47	44.65	6.00
rc205c10-s4	2	334.54	330.55	2	380.39	364.59	27.55	13.70	–	INF			–
Avg.	2.17	326.11	313.96	2.25	343.10	325.67	16.13	5.45	2.11	351.02	322.65	40.81	9.56
r102c15-s8	5	430.83	420.10	5	418.58	406.54	6.28	-2.84	–	INF			–
r105c15-s6	4	350.09	336.15	4	403.60	387.95	29.76	15.28	–	INF			–
r202c15-s6	1	590.31	565.53	**2**	406.51	389.72	29.26	–	**2**	437.63	423.42	19.23	–
r209c15-s5	1	347.31	333.50	1	355.35	338.37	13.36	2.32	**2**	368.31	352.98	25.85	–
c103c15-s5	3	401.97	376.26	3	400.90	373.63	14.33	-0.27	**4**	464.61	425.18	52.07	–
c106c15-s3	3	352.29	336.79	3	311.09	295.36	10.70	-11.69	3	371.22	342.63	47.09	5.37
c202c15-s5	2	393.19	383.62	2	449.40	415.69	55.12	14.30	2	534.02	478.35	106.41	35.82
c208c15-s4	2	310.12	300.55	2	415.93	395.59	13.57	34.12	**3**	436.05	418.33	16.99	–
rc103c15-s5	4	415.79	397.67	4	447.13	432.28	1.59	7.54	–	INF			–
rc108c15-s5	3	417.92	389.13	3	434.80	409.39	5.56	4.04	–	INF			–
rc202c15-s5	2	403.03	394.39	2	416.91	407.20	3.33	3.44	2	431.81	406.64	41.07	7.14
rc204c15-s7	1	402.15	385.01	1	423.30	399.35	11.85	5.26	1	483.75	455.13	19.51	20.29
Avg.	2.58	401.25	384.89	2.67	406.96	387.59	16.23	6.50	2.38	440.93	412.83	41.03	17.16
Total Avg.	2.06	308.53	297.00	2.11	319.61	305.16	12.00	5.88	1.97	341.46	319.35	33.00	16.21

The most substantial energy savings are observed in "r102c10-s4" with a 2.3% reduction. On the other hand, the highest increase in energy consumption occurs in "c206c5-s4", with a 49% rise. We also observe that road gradients can influence the frequency of EVs' recharging station visits along the routes. Regenerative braking on downhill roads may allow EVs to bypass some stations, while traveling uphill may require more frequent stops at stations due to increased consumption. In the *Nearly Level* case, EVs visit recharging stations 2% more often on average compared to the *Level* case. As the road gradient increases, this frequency rises. Specifically, in the *Very Gentle Slope* case, EVs visit recharging stations 28% more frequently on average compared to the *Level* case, considering the solutions with the same number of

vehicles. We observe that the tours change in the presence of road gradients, as indicated by the differences in total distances traveled. In only two instances, "c202c10-s5" and "c205c10-s3", the routes for the *Level* and *Nearly Level* cases remain the same (indicated in bold in the "*Dist*" column). However, in both instances, energy consumption increases as the network becomes steeper.

4.3.1. Influence of ignoring road gradients in route planning

The results presented in Table 7 suggest that considering road gradients not only affect the total energy consumption, but also how the routes are formed. We further investigate how route plans change using two instances, "c106c15" and "c208c15," by comparing the solutions of the *Level* and *Nearly-Level* cases. In the "c106c15" instance, considering road gradients results in a solution with 11.7% lower total energy consumption than that obtained assuming a flat network. Figure 6 illustrates these solutions, which exhibit different routes. The solid and dashed arcs represent the roads with positive and negative gradients, respectively. In Route 1' depicted in Figure 6.b, the EV recharges along the downhill paths, S15→C68→C64, S19→C78, and C84→C89→C91→Depot, which helps to achieve a more energy-efficient route. However, this route becomes energy-infeasible if road gradients are ignored, as the battery cannot benefit from these savings. Hence, when the gradients are considered, the routes are formed so that the regenerative braking is utilized effectively.

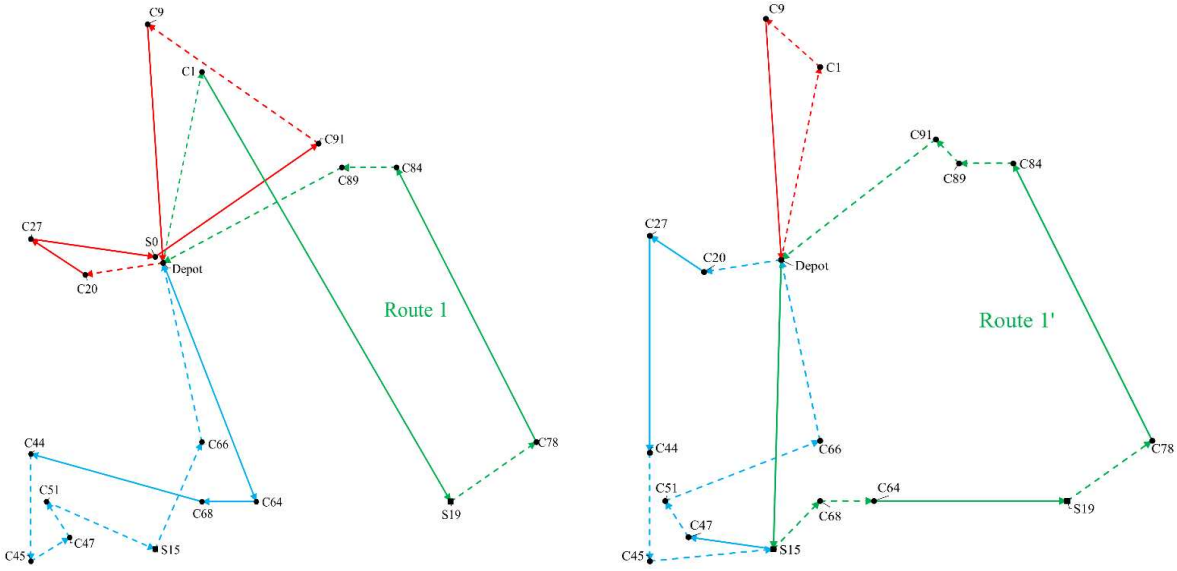

(a) *Level* road network (Energy: 352.29) (b) *Nearly Level* road network (Energy: 311.09)

Figure 6. Comparison of "c106c15" solutions with different road network topographies

Conversely, in the "c208c15", when the road gradients are ignored (*Level* road network) the EVs consume 34.1% lower total energy than those of the *Nearly-Level* case, which are depicted in Figure 7. These solutions also demonstrate that, contrary to the previous case, customers might be visited in the same order,

but different recharging decisions might be required. For example, in this solution, the routes remain largely unchanged except for the addition of S1 at the end of Route 1 between C75 and the depot.

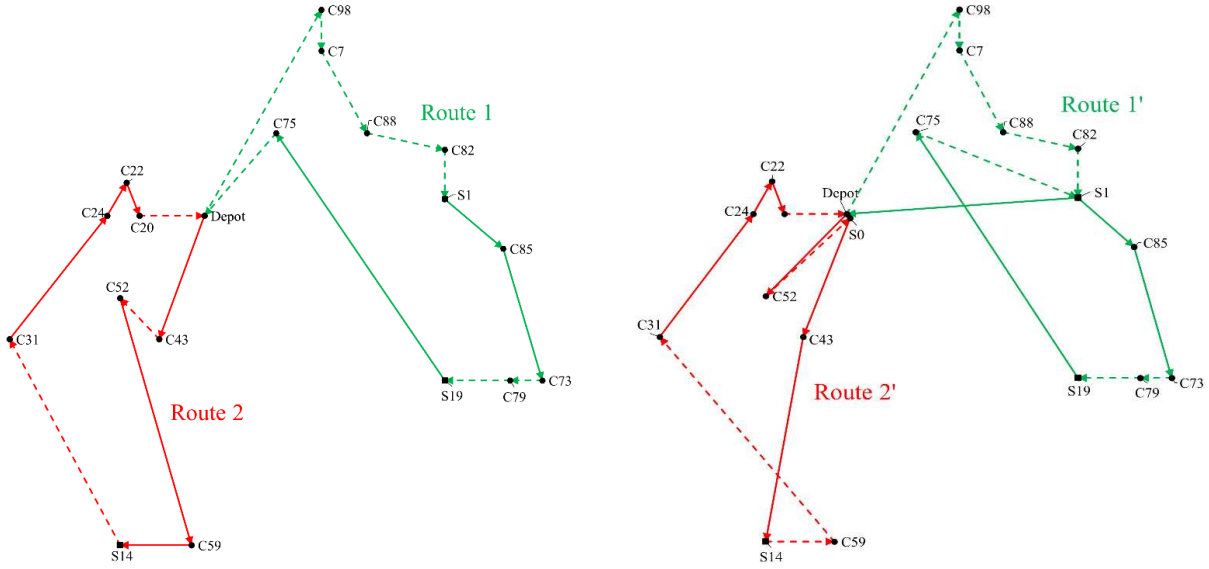

(a) *Level* road network (Energy: 310.12) (b) *Nearly-Level* road network (Energy: 415.93)

Figure 7. Comparison of optimal solutions for "c208c15" on different road network topographies

We also show how the energy would be consumed if the vehicle follows the route obtained ignoring the gradients. Route 2 on the *Level* road network shown in Figure 7.a is illustrated on a *Nearly-Level* road network in Figure 8, where the arcs are drawn according to whether they are downhill and uphill with angles proportional to road gradients shown in parentheses where the values are in percentages. The values on top of the nodes in green, represent the remaining energy in the battery upon arriving at that node. It is evident that the route becomes infeasible while traveling from C59 to S14, as there are several uphill roads. Therefore, in Route 2', C52 and C43 are swapped, and another station is visited in between to compensate the high energy consumption until reaching S14, which is also visited before C59 to take advantage of the regenerative braking between them.

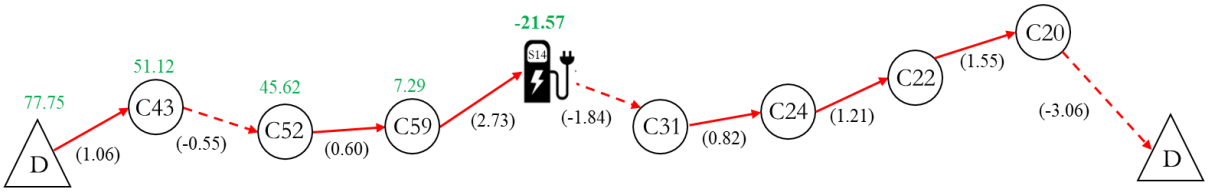

Figure 8. Energy profiles of Route 2 in Figure 7.a on *Nearly-Level* road network

4.3.2. Influence of the depot's altitude in route planning

We conducted additional experiments to observe the effect of depot altitude on routing decisions, analyzing

scenarios where the depot is located at either a higher or lower altitude. Our results also show that considering the network topography may help decision-makers in selecting their depot locations.

Table 8 demonstrates the impact of depot altitude on total energy consumption where the first column represents the depot's altitude. The "Base Case" refers to the solutions obtained for the pickup problem in the *Nearly-Level* case, where the depot altitude remains unchanged at zero. Two instances, "c106c15-s3" and "rc202c15-s5", are analyzed, where the average and maximum altitude of the nodes in the network for the base case (average, max) are (0.23, 0.63) and (0.27, 0.75), respectively. The amount of regenerated energy through regenerative braking process for each instance is presented in column "*Reg*". We then explored additional scenarios, adjusting the depot's altitude either below or above the base case, with the specific altitude values provided in the first column of Table 8. The results suggest that an increase in depot altitude compared to the base case leads to a corresponding rise in energy consumption if the routes are the same or similar. This is due to EVs traveling on positive road gradients back to the depot loaded with heavy loads which increases the energy consumption. On the other hand, when the depot's altitude decreases compared to the base case, if the routes remain unchanged or only slightly altered, negative gradients can reduce energy consumption, as the EVs return loaded and benefit from downhill travel. However, beyond a certain decrease in altitude, the existing routes become infeasible, resulting in route changes and subsequent increases in energy consumption. This explains the U-shaped behavior of the energy consumption observed in Figures 9.a and 9.b.

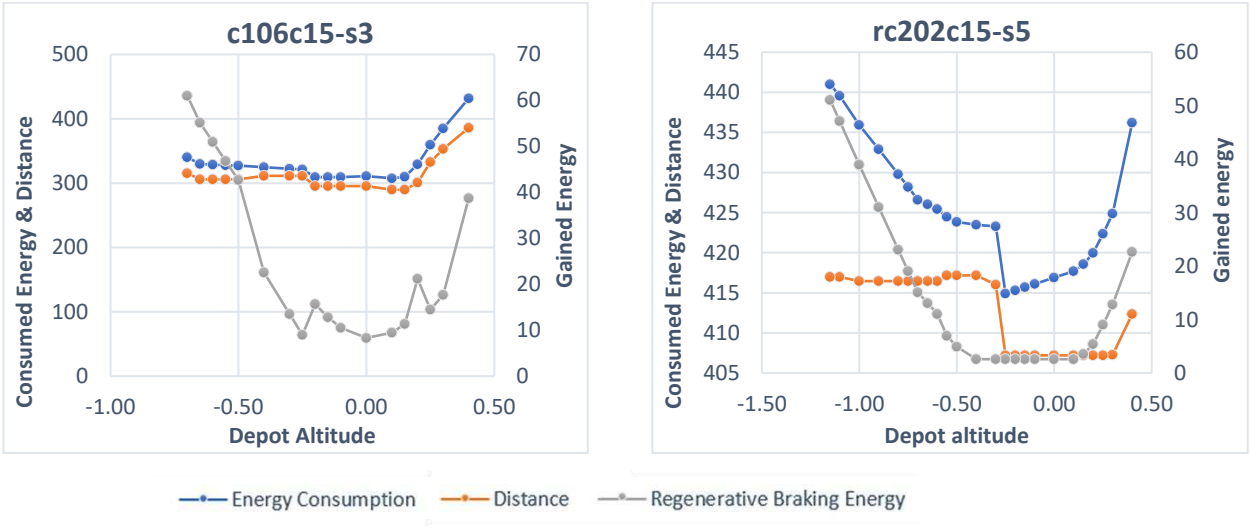

(a) Effect of depot altitude on energy consumption in "c106c15-s3"

(b) Effect of depot altitude on energy consumption in "rc202c15-s5"

Figure 9. Influence of the depot's altitude in route planning

Table 8. Analysis of depot altitude and its impact on the total energy consumption of an EV fleet

	c106c15-s3					rc202c15-s5				
Altitude	*#Veh*	*EC*	*Dist*	*Reg*	*%ΔEC*	*#Veh*	*EC*	*Dist*	*Reg*	*%ΔEC*
0.70	15		INF			15		INF		
0.65	4	506.89	439.04	63.02	62.94	3	665.43	638.29	21.87	59.61
0.60	4	423.51	369.54	48.58	36.14	3	662.99	638.29	18.17	59.02
0.55	4	419.04	369.54	43.00	34.70	3	627.29	596.43	31.42	50.46
0.50	4	414.58	369.54	37.42	33.27	3	582.40	555.47	27.65	39.70
0.40	3	431.65	385.80	38.70	38.75	2	436.22	412.36	22.66	4.63
0.30	3	385.03	352.94	17.69	23.77	2	424.87	407.29	12.80	1.91
0.25	3	359.70	332.83	14.46	15.62	2	422.37	407.20	9.07	1.31
0.20	3	329.45	301.00	21.18	5.90	2	419.98	407.20	5.38	0.74
0.15	3	310.02	289.72	11.34	-0.34	2	418.58	407.20	3.52	0.40
0.10	3	307.60	289.72	9.47	-1.12	2	417.68	407.20	2.59	0.19
0.00	3	311.09	295.36	8.32	0.00	2	416.91	407.20	2.59	0.00
-0.10	3	309.46	295.36	10.49	-0.52	2	416.12	407.20	2.59	-0.19
-0.15	3	309.30	295.36	12.79	-0.58	2	415.71	407.20	2.59	-0.29
-0.20	3	309.47	295.36	15.69	-0.52	2	415.30	407.20	2.59	-0.38
-0.25	3	321.38	311.51	8.97	3.31	2	414.89	407.20	2.59	-0.48
-0.30	3	322.44	311.51	13.51	3.65	2	423.28	416.01	2.59	1.53
-0.40	3	324.56	311.51	22.58	4.33	2	423.50	417.17	2.59	1.58
-0.50	3	327.05	305.88	42.66	5.13	2	423.84	417.17	4.94	1.66
-0.55	3	327.90	305.88	46.82	5.40	2	424.46	417.17	6.98	1.81
-0.60	3	328.75	305.88	50.98	5.68	2	425.44	416.45	11.03	2.05
-0.65	3	329.60	305.88	55.13	5.95	2	426.02	416.45	13.07	2.19
-0.70	3	340.21	315.20	61.02	9.36	2	426.59	416.45	15.10	2.32
-0.75	4	357.33	332.48	66.64	14.86	2	428.18	416.45	19.05	2.70
-0.80	15		INF			2	429.77	416.45	23.03	3.09
-0.90						2	432.89	416.45	31.00	3.83
-1.00						2	435.92	416.45	38.96	4.56
-1.10						2	439.56	416.99	47.08	5.43
-1.15						2	440.99	416.99	51.06	5.78
-1.20						15		INF		

As shown in Table 8, if depot is located in very low/high altitude, it can result in a higher number of vehicles or even make the problem infeasible. In extreme cases in the "c106c15-s3" and "rc202c15-s5" instances, the number of vehicles increases by one, and energy consumption rises by up to 63% and 60%, respectively. However, if the depot is located slightly at low altitude, energy consumption can decrease by 0.58% and 0.48% for "c106c15-s3" and "rc202c15-s5", respectively. In both instances, the energy consumption increases more significantly when the depot altitude is raised compared to when it is lowered. Moreover, as indicated in Table 8, and Figures 9.a and 9.b, the amount of regenerated energy generally follows a U-shaped pattern, increasing as the depot is in extremely low or high altitude resulting in having steeper roads.

It has been observed that in scenarios where vehicles pick up goods from customers and have the option to return fully loaded to the depot, it may be advantageous to locate the depot at a lower altitude. This enables the fully loaded vehicle to travel downhill, utilizing regenerative braking to save energy. However, due to the observed U-shaped pattern in energy consumption, careful examination is required, as selecting a depot at a very low altitude can lead to an increase in energy consumption. Conversely, in scenarios where EVs

deliver goods and return to the depot empty, locating the depot at a higher altitude (up to a certain point, as dictated by the U-shaped pattern) may be more favorable. In this case, the EVs can regenerate energy during their descent while carrying a full load at the beginning of their route.

5. Discussion and Conclusion

In this study, we investigated the effects of road gradients, regenerative braking, and cargo weights on the routing decisions in EVRPTW using a partial recharging strategy. We introduced the mathematical model of the problem, but due to the inherent nonlinearity and intractability of this model, we proposed three different MILP models to address these challenges. While one of these replaces the nonlinear energy consumption with a linear approximation to calculate the total consumption, the other models calculate the exact energy consumptions. We introduced a new dataset by assigning altitudes to the nodes of existing benchmark instances in the literature using *k*-means algorithm to ensure consistency. Using this dataset, we compared the performances of the proposed models. The model using the approximation was not always accurate, e.g., in some instances it provided infeasible or worse solutions compared to those obtained by the other models. Among the proposed models, MILP2, which uses the flow variables to calculate the objective function, is both accurate and fast, finding the optimal solutions in 35 of the 36 instances in 67 seconds on average.

Using this model, extensive computational tests were conducted across three different network configurations based on their average absolute road gradients. The results indicated that considering road gradients and regenerative braking alongside cargo loads significantly impacts routing decisions. Some instances became infeasible with the introduction of road gradients due to the battery capacity being not sufficient to travel on some arcs. In some instances, the total energy consumption increased by up to 49% due to the steep roads leading to more consumption, and thus more visits to recharging stations, resulting in several detours. In some of these cases, the fleet size was forced to increase to ensure feasibility. On the other hand, in some instances total energy consumption reduced by up to 11.7% by taking advantage of regenerative braking, especially while carrying a heavy load downhill. We also observed that when road gradients were considered, in the majority of the instances, the routes changed to comply with the minimum energy requirement depending on the altitude of the customers and the depot.

These results shed light on the strategic, tactical, and operational decisions in logistics operations. The companies should consider the topography of the network they operate while deciding the fleet size and mix, e.g., they might prefer a mixed fleet including diesel or hybrid vehicles if servicing the customers with an EV fleet is not possible due to steep roads. The optimal combination of different powertrain options will depend on operational requirements, regional climate conditions, and the road network. Hence, designing

the optimal fleet and routes for different regions presents a complex challenge that warrants further study. Furthermore, the location of the depot is quite important if the network comprises steep roads, and this may open a future research direction to combine location and routing decisions. Finally, the arcs in this study are assumed shortest paths between two points, and the gradient of this path is assumed fixed on this arc, i.e., an average slope is considered. However, the paths may include arcs with very different gradients. Therefore, another future research may be directed towards including precise gradients of each connection in the network, utilizing multi-graph approaches. Furthermore, it worth investigating time-dependency in the EVRPTW, where varying traffic conditions impose different speed levels at different times of the day, which may affect energy consumption and consequently routing decisions. Finally, this study focused on modeling the EVRPTW considering cargo load, road gradients and regenerative braking, and the experiments were based on solving instances by a solver. Our experiments showed a significant increase in computational time and optimality gap as the problem size increases, particularly highlighting the difficulty of obtaining optimal solutions with minimal EV fleet size. Developing tailored solution methodologies to solve large instances, preferably based on real-life data is another potential direction for future research.

Source code and data availability

The source code and detailed solution outputs are publicly available on GitHub (https://github.com/sinarastani/EVRPTW-GR). The datasets used in this study are available via Mendeley Data (https://data.mendeley.com/datasets/srfdbp2twv/1).

References

Akbari, V., Çatay, B. and Sadati, İ., 2024. Route optimization of battery electric vehicles using dynamic charging on electrified roads. Sustainable Cities and Society, 109, p.105532.

Asamer, J., Graser, A., Heilmann, B. and Ruthmair, M., 2016. Sensitivity analysis for energy demand estimation of electric vehicles. Transportation Research Part D: Transport and Environment, 46, pp.182-199.

Barth, M. and Boriboonsomsin, K., 2009. Energy and emissions impacts of a freeway-based dynamic eco-driving system. Transportation Research Part D: Transport and Environment, 14(6), pp.400-410.

Barth, M., Younglove, T. and Scora, G., 2005. Development of a heavy-duty diesel modal emissions and fuel consumption model. UC Berkeley: California Partners for Advanced Transportation Technology. Available at: https://escholarship.org/uc/item/67f0v3zf (Accessed: 4 July 2025).

Basso, R., Kulcsár, B. and Sanchez-Diaz, I., 2021. Electric vehicle routing problem with machine learning for energy prediction. Transportation Research Part B: Methodological, 145, pp.24-55.

Basso, R., Kulcsár, B., Egardt, B., Lindroth, P. and Sanchez-Diaz, I., 2019. Energy consumption estimation integrated into the electric vehicle routing problem. Transportation Research Part D: Transport and Environment, 69, pp.141-167.

Bragin, M.A., Ye, Z. and Yu, N., 2024. Toward efficient transportation electrification of heavy-duty trucks: Joint scheduling of truck routing and charging. Transportation Research Part C: Emerging Technologies, 160, p.104494.

Bruglieri, M., Çatay B, Keskin M, Mancini, S., and Pisacane, O., 2025. The mixed-fleet vehicle routing problem with low emission zones. Transportation Research Part E: Logistics and Transportation Review, 201, p.104230.

Bruglieri, M., Mancini, S. and Pisacane, O., 2021. A more efficient cutting planes approach for the green vehicle routing problem with capacitated alternative fuel stations. Optimization Letters, pp.1-17.

Bruglieri, M., Mancini, S., Pezzella, F. and Pisacane, O., 2016. A new mathematical programming model for the green vehicle routing problem. Electronic Notes in Discrete Mathematics, 55, pp.89-92.

Bruglieri, M., Paolucci, M. and Pisacane, O., 2023. A matheuristic for the electric vehicle routing problem with time windows and a realistic energy consumption model. Computers & Operations Research, 157, p.106261.

Bruglieri, M., Pezzella, F., Pisacane, O. and Suraci, S., 2015. A variable neighborhood search branching for the electric vehicle routing problem with time windows. Electronic Notes in Discrete Mathematics, 47, pp.221-228.

Çalık, H., Oulamara, A., Prodhon, C. and Salhi, S., 2021. The electric location-routing problem with heterogeneous fleet: Formulation and Benders decomposition approach. Computers & Operations Research, 131, p.105251.

Çatay, B. and Sadati, İ., 2023. An improved matheuristic for solving the electric vehicle routing problem with time windows and synchronized mobile charging/battery swapping. Computers & Operations Research, 159, p.106310.

Conrad, R.G. and Figliozzi, M.A., 2011. The recharging vehicle routing problem. Proceedings of the 2011 Industrial Engineering Research Conference, vol. 8, IISE, Norcross, GA.

Dastpak, M., Errico, F., Jabali, O. and Malucelli, F., 2024. Dynamic routing for the Electric Vehicle Shortest Path Problem with charging station occupancy information. Transportation Research Part C: Emerging Technologies, 158, p.104411.

Demir, E., Bektaş, T. and Laporte, G., 2011. A comparative analysis of several vehicle emission models

for road freight transportation. Transportation Research Part D: Transport and Environment, 16(5), pp.347-357.

Desaulniers, G., Errico, F., Irnich, S. and Schneider, M., 2016. Exact algorithms for electric vehicle-routing problems with time windows. Operations Research, 64(6), pp.1388-1405.

Dolgui, A., Kovalev, S. and Kovalyov, M.Y., 2024. Scheduling electric vehicle regular charging tasks: A review of deterministic models. European Journal of Operational Research, 325(2), pp.221-232.

Duman, E.N., Taş, D. and Çatay, B., 2022. Branch-and-price-and-cut methods for the electric vehicle routing problem with time windows. International Journal of Production Research, 60(17), pp.5332-5353.

Erdelić, T. and Carić, T., 2019. A survey on the electric vehicle routing problem: variants and solution approaches. Journal of Advanced Transportation, 2019(1), p.5075671.

Erdoğan, B., Tural, M.K. and Khoei, A.A., 2023. Finding an energy efficient path for plug-in electric vehicles with speed optimization and travel time restrictions. Computers & Industrial Engineering, 176, p.108987.

Erdoğan, S. and Miller-Hooks, E., 2012. A green vehicle routing problem. Transportation Research Part E: Logistics and Transportation Review, 48(1), pp.100-114.

Felipe, Á., Ortuño, M.T., Righini, G. and Tirado, G., 2014. A heuristic approach for the green vehicle routing problem with multiple technologies and partial recharges. Transportation Research Part E: Logistics and Transportation Review, 71, pp.111-128.

Fiori, C., Ahn, K. and Rakha, H.A., 2016. Power-based electric vehicle energy consumption model: Model development and validation. Applied Energy, 168, pp.257-268.

Froger, A., Jabali, O., Mendoza, J.E. and Laporte, G., 2022. The electric vehicle routing problem with capacitated charging stations. Transportation Science, 56(2), pp.460-482.

GCELAB (2020) Road Gradient Types: Cycle Track Gradient. Available at: https://www.gcelab.com/blog/road-gradient-types-cycle-track-gradient#:~:text=The%20type%20of%20Road%20directly,desirable%20maximum%20gradient%20is%206%25 (Accessed: 4 July 2025).

Geography Fieldwork (2024) Slope Steepness Index. Available at: https://geographyfieldwork.com/SlopeSteepnessIndex.htm (Accessed: 7 November 2024).

Goeke, D. and Schneider, M., 2015. Routing a mixed fleet of electric and conventional vehicles. European Journal of Operational Research, 245(1), pp.81-99.

Guo, F., Zhang, J., Huang, Z. and Huang, W., 2022. Simultaneous charging station location-routing

problem for electric vehicles: Effect of nonlinear partial charging and battery degradation. Energy, 250, p.123724.

Gutierrez-Alcoba, A., Rossi, R., Martin-Barragan, B. and Embley, T., 2023. The stochastic inventory routing problem on electric roads. European Journal of Operational Research, 310(1), pp.156-167.

Hiermann, G., Hartl, R.F., Puchinger, J. and Vidal, T., 2019. Routing a mix of conventional, plug-in hybrid, and electric vehicles. European Journal of Operational Research, 272(1), pp.235-248.

Jie, W., Yang, J., Zhang, M. and Huang, Y., 2019. The two-echelon capacitated electric vehicle routing problem with battery swapping stations: Formulation and efficient methodology. European Journal of Operational Research, 272(3), pp.879-904.

Kancharla, S.R. and Ramadurai, G., 2018. An adaptive large neighborhood search approach for electric vehicle routing with load-dependent energy consumption. Transportation in Developing Economies, 4, pp.1-9.

Kancharla, S.R. and Ramadurai, G., 2020. Electric vehicle routing problem with non-linear charging and load-dependent discharging. Expert Systems with Applications, 160, p.113714.

Keskin, M. and Çatay, B., 2016. Partial recharge strategies for the electric vehicle routing problem with time windows. Transportation research part C: Emerging Technologies, 65, pp.111-127.

Keskin, M. and Çatay, B., 2018. A matheuristic method for the electric vehicle routing problem with time windows and fast chargers. Computers & operations research, 100, pp.172-188.

Keskin, M., Çatay, B. and Laporte, G., 2021. A simulation-based heuristic for the electric vehicle routing problem with time windows and stochastic waiting times at recharging stations. Computers & Operations Research, 125, p.105060.

Keskin, M., Laporte, G. and Çatay, B., 2019. Electric vehicle routing problem with time-dependent waiting times at recharging stations. Computers & Operations Research, 107, pp.77-94.

Kucukoglu, I., Dewil, R. and Cattrysse, D., 2021. The electric vehicle routing problem and its variations: A literature review. Computers & Industrial Engineering, 161, p.107650.

Kullman, N.D., Goodson, J.C. and Mendoza, J.E., 2021. Electric vehicle routing with public charging stations. Transportation Science, 55(3), pp.637-659.

Lam, E., Desaulniers, G. and Stuckey, P.J., 2022. Branch-and-cut-and-price for the electric vehicle routing problem with time windows, piecewise-linear recharging and capacitated recharging stations. Computers & Operations Research, 145, p.105870.

Li, Y., Xu, X., Shao, H., Song, X. and Shen, L., 2024. Finding the optimal reliable energy consumption

path for electric vehicles under rainfall conditions. Transportmetrica B: Transport Dynamics, 12(1), p.2352492.

Liu, Z., Zuo, X., Zhou, M., Guan, W. and Al-Turki, Y., 2023. Electric vehicle routing problem with variable vehicle speed and soft time windows for perishable product delivery. IEEE Transactions on Intelligent Transportation Systems, 24(6), pp.6178-6190.

Lowell, J., 2020. EVs: Are they really more efficient? Australian Energy Council. Available at: https://www.energycouncil.com.au/analysis/evs-are-they-really-more-efficient/#_ednref3 (Accessed: 4 July 2025).

Ma, T.Y., Fang, Y., Connors, R.D., Viti, F. and Nakao, H., 2024. A hybrid metaheuristic to optimize electric first-mile feeder services with charging synchronization constraints and customer rejections. Transportation Research Part E: Logistics and Transportation Review, 185, p.103505.

Macrina, G., Pugliese, L.D.P., Guerriero, F. and Laporte, G., 2019. The green mixed fleet vehicle routing problem with partial battery recharging and time windows. Computers & Operations Research, 101, pp.183-199.

Marra, F., Yang, G.Y., Træholt, C., Larsen, E., Rasmussen, C.N. and You, S., 2012. Demand profile study of battery electric vehicle under different charging options. In *2012 IEEE power and energy society general meeting* (pp. 1-7).

Montoya, A., Guéret, C., Mendoza, J.E. and Villegas, J.G., 2017. The electric vehicle routing problem with nonlinear charging function. Transportation Research Part B: Methodological, 103, pp.87-110.

Park, H. and Lee, C., 2024. An exact algorithm for maximum electric vehicle flow coverage problem with heterogeneous chargers, nonlinear charging time and route deviations. European Journal of Operational Research, 315(3), pp.926-951.

Pelletier, S., Jabali, O., Laporte, G. and Veneroni, M., 2017. Battery degradation and behaviour for electric vehicles: Review and numerical analyses of several models. Transportation Research Part B: Methodological, 103, pp.158-187.

Raeesi, R. and Zografos, K.G., 2022. Coordinated routing of electric commercial vehicles with intra-route recharging and en-route battery swapping. European Journal of Operational Research, 301(1), pp.82-109.

Rastani, S. and Çatay, B., 2023. A large neighborhood search-based matheuristic for the load-dependent electric vehicle routing problem with time windows. Annals of Operations Research, 324, 761–793.

Rastani, S., Yüksel, T. and Çatay, B., 2019. Effects of ambient temperature on the route planning of electric freight vehicles. Transportation Research Part D: Transport and Environment, 74, pp.124-141.

Sadati, M.E.H., Akbari, V. and Çatay, B., 2022. Electric vehicle routing problem with flexible deliveries. International Journal of Production Research, 60(13), pp.4268-4294.

Schiffer, M. and Walther, G., 2018. An adaptive large neighborhood search for the location-routing problem with intra-route facilities. Transportation Science, 52(2), pp.331-352.

Schneider, M., Stenger, A. and Goeke, D., 2014. The electric vehicle-routing problem with time windows and recharging stations. Transportation Science, 48(4), pp.500-520.

Solomon, M.M., 1987. Algorithms for the vehicle routing and scheduling problems with time window constraints. Operations Research, 35(2), pp.254-265.

Souza, A.L., Papini, M., Penna, P.H. and Souza, M.J., 2024. A flexible variable neighbourhood search algorithm for different variants of the Electric Vehicle Routing Problem. Computers & Operations Research, p.106713.

Soysal, M., Çimen, M. and Belbağ, S., 2020. Pickup and delivery with electric vehicles under stochastic battery depletion. Computers & Industrial Engineering, 146, p.106512.

Sun, H., Wu, T., Bai, Q. and Zhou, Z., 2025. Improved adaptive large-scale neighborhood search algorithm for electric vehicle routing problem with soft time windows and linear weight-related discharging. Expert Systems with Applications, 280, p.127344.

Sweda, T.M., Dolinskaya, I.S. and Klabjan, D., 2017. Adaptive routing and recharging policies for electric vehicles. Transportation Science, 51(4), pp.1326-1348.

Wang, W. and Zhao, J., 2023. Partial linear recharging strategy for the electric fleet size and mix vehicle routing problem with time windows and recharging stations. European Journal of Operational Research, 308(2), pp.929-948.

Wang, X., Liang, Y., Tang, X. and Jiang, X., 2023. A multi-compartment electric vehicle routing problem with time windows and temperature and humidity settings for perishable product delivery. Expert Systems with Applications, 233, p.120974.

Wu, X., Freese, D., Cabrera, A. and Kitch, W.A., 2015. Electric vehicles' energy consumption measurement and estimation. Transportation Research Part D: Transport and Environment, 34, pp.52-67.

Xiao, Y., Zhang, Y., Kaku, I., Kang, R. and Pan, X., 2021. Electric vehicle routing problem: A systematic review and a new comprehensive model with nonlinear energy recharging and consumption. Renewable and Sustainable Energy Reviews, 151, p.111567.

Xiao, Y., Zuo, X., Kaku, I., Zhou, S. and Pan, X., 2019. Development of energy consumption optimization model for the electric vehicle routing problem with time windows. Journal of Cleaner Production, 225,

pp.647-663.

Xu, G., Li, W., Xu, K. and Song, Z., 2011. An intelligent regenerative braking strategy for electric vehicles. Energies, 4(9), pp.1461-1477.

Yamín, D., Desaulniers, G. and Mendoza, J.E., 2024. The electric vehicle routing and overnight charging scheduling problem on a multigraph. INFORMS Journal on Computing.

Yang, J. and Sun, H., 2015. Battery swap station location-routing problem with capacitated electric vehicles. Computers & Operations Research, 55, pp.217-232.

Zang, Y., Wang, M. and Qi, M., 2022. A column generation tailored to electric vehicle routing problem with nonlinear battery depreciation. Computers & Operations Research, 137, p.105527.

Zhang, L., Wang, S. and Qu, X., 2021. Optimal electric bus fleet scheduling considering battery degradation and non-linear charging profile. Transportation Research Part E: Logistics and Transportation Review, 154, p.102445.

Zhang, S., Gajpal, Y., Appadoo, S.S. and Abdulkader, M.M.S., 2018. Electric vehicle routing problem with recharging stations for minimizing energy consumption. International journal of production economics, 203, pp.404-413.

Zhang, S., Zhou, S., Luo, R., Zhao, R., Xiao, Y. and Xu, Y., 2023. A low-carbon, fixed-tour scheduling problem with time windows in a time-dependent traffic environment. International Journal of Production Research, 61(18), pp.6177-6196.

Zhang, S., Zhou, T., Fang, C. and Yang, S., 2024. A novel collaborative electric vehicle routing problem with multiple prioritized time windows and time-dependent hybrid recharging. Expert Systems with Applications, 244, p.122990.